

Southern NT, Northern Territory  
TEMPEST  
Geophysical Survey

Acquisition and Processing Report  
for

Toro Energy Limited  
Scimitar Resources Limited

Prepared by : M. Lawrence .....

L. Stenning .....

Authorised for release by : .....

.....

Survey flown: July 2007

by



*Fugro Airborne Surveys*  
65 Brockway Road, Floreat. WA 6014, Australia  
Tel: (61-8) 9273 6400 Fax: (61-8) 9273 6466

**FAS JOB # 1900**

## CONTENTS

<b>1. SURVEY OPERATIONS AND LOGISTICS.....</b>	<b>4</b>
1.1 INTRODUCTION.....	4
1.2 SURVEY BASE .....	4
1.3 SURVEY PERSONNEL .....	4
1.4 AREA MAP .....	5
<b>2. SURVEY SPECIFICATIONS AND PARAMETERS.....</b>	<b>6</b>
2.1 AREA CO-ORDINATES .....	6
2.2 SURVEY AREA PARAMETERS .....	6
2.3 FLIGHT PLANS .....	6
2.4 JOB SAFETY PLAN.....	7
<b>3. AIRCRAFT EQUIPMENT AND SPECIFICATIONS.....</b>	<b>8</b>
3.1 AIRCRAFT.....	8
3.2 TEMPEST SYSTEM SPECIFICATIONS .....	8
3.2.1 EM Receiver and Logging Computer .....	8
3.2.2 TEMPEST Transmitter .....	9
3.2.3 TEMPEST 3-Axis Towed Bird Assembly .....	9
3.3 PDAS 1000 SURVEY COMPUTER .....	9
3.3.1 Cesium Vapour Magnetometer Sensor .....	9
3.3.2 Magnetometer Processor Board .....	9
3.3.3 Fluxgate Magnetometer .....	9
3.3.4 GPS Receiver.....	9
3.3.5 Differential GPS Demodulator .....	9
3.4 NAVIGATION SYSTEM .....	10
3.5 ALTIMETER SYSTEM.....	10
3.5.1 Radar Altimeter .....	10
3.5.2 Barometric Altimeter.....	10
3.6 VIDEO TRACKING SYSTEM.....	10
3.7 DATA RECORDED BY THE AIRBORNE ACQUISITION EQUIPMENT .....	10
<b>4. GROUND DATA ACQUISITION EQUIPMENT AND SPECIFICATIONS .....</b>	<b>11</b>
4.1 MAGNETIC BASE STATION.....	11
4.2 GPS BASE STATION .....	11
<b>5. EM AND OTHER CALIBRATIONS AND MONITORING .....</b>	<b>12</b>
5.1 PRE-FLIGHT BAROMETER CALIBRATION: LINE C1511.....	12
5.2 PRE-FLIGHT ZERO: LINE C9001.....	12
5.3 PRE-FLIGHT SWOOPS: LINE C9002.....	12
5.4 POST-FLIGHT ZERO: LINE C9003.....	12
5.5 POST-FLIGHT BAROMETER CALIBRATION: LINE C1611.....	12
5.6 ADDITIVE EM MEASUREMENTS: LINES C9004, C9005, AND C9007 .....	12
5.7 DYNAMIC MAGNETOMETER COMPENSATION.....	12
5.8 PARALLAX CHECKS .....	13
5.9 RADAR ALTIMETER CALIBRATION.....	13
5.10 HEADING ERROR CHECKS.....	13
<b>6. DATA PROCESSING .....</b>	<b>14</b>
6.1 FIELD DATA PROCESSING .....	14
6.1.1 Quality Control Specifications .....	14
6.1.2 In-Field Data Processing .....	14
6.2 FINAL DATA PROCESSING .....	14
6.2.1 Magnetics .....	14
6.2.2 Derived Topography.....	15
6.2.3 Electromagnetic Data Processing .....	16

6.2.4	Conductivity Depth Images (CDI).....	19
6.2.5	System Specifications for Modelling TEMPEST Data.....	19
6.2.6	Delivered Products .....	20
<b>7.</b>	<b>REFERENCES .....</b>	<b>21</b>
	<b>APPENDIX I – FLIGHT PLAN .....</b>	<b>22</b>
	<b>APPENDIX II – WEEKLY ACQUISITION REPORTS .....</b>	<b>23</b>
	<b>APPENDIX III – FLIGHT SUMMARY (LINE LISTING) .....</b>	<b>24</b>
	<b>APPENDIX IV – LOCATED DATA FORMAT .....</b>	<b>25</b>
	<b>APPENDIX V – LIST OF ALL SUPPLIED DATA AND PRODUCTS .....</b>	<b>42</b>

## **1. SURVEY OPERATIONS AND LOGISTICS**

### **1.1 Introduction**

On the 18<sup>th</sup> of July 2007, Fugro Airborne Surveys Pty. Ltd. (FAS) undertook an airborne TEMPEST electromagnetic and magnetic survey for Toro Energy Limited and Scimitar Resources Limited, over the Southern NT Project area in the Northern Territory. The survey was flight planned as one area, due to lines covering both company's tenements. The data was acquired and processed as one contiguous block and split into areas at the final processing stage. Total coverage of the survey amounted to 550 line kilometres flown in 2 flights. The survey was flown using a CASA C212-200 Turbo Prop aircraft, registration VH-TEM owned and operated by FAS. This report summarises the procedures and equipment used by FAS in the acquisition, verification and processing of the airborne geophysical data.

### **1.2 Survey Base**

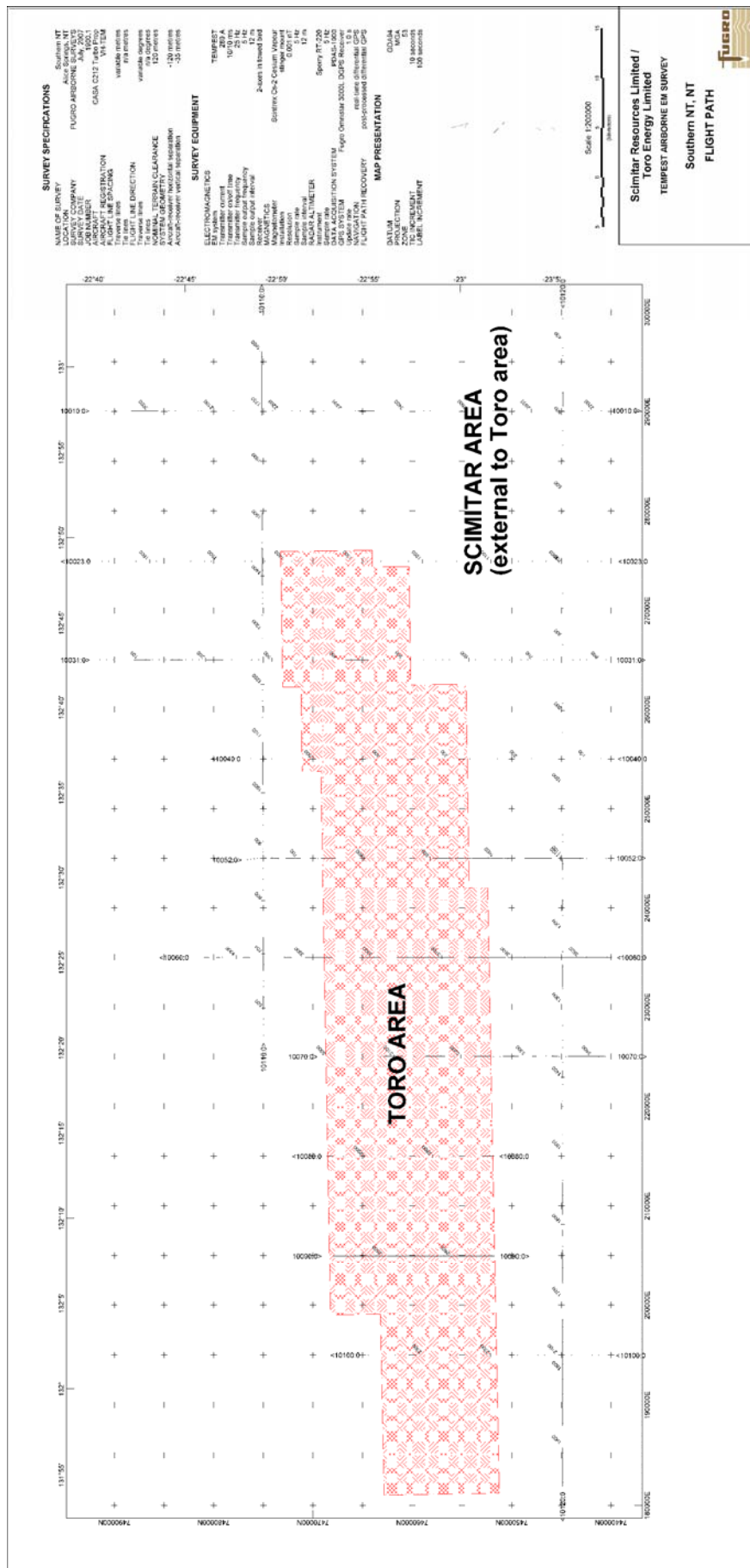
The survey was based out of Alice Springs, Northern Territory. The survey aircraft was operated from the Alice Springs airport with the aircraft fuel available on site. A temporary office was set up at the airport, where all survey operations were run and the post-flight data verification was performed.

### **1.3 Survey Personnel**

The following personnel were involved in this project:

Project Supervision - Acquisition	Bart Anderson
- Processing	Matthew Owers
On-site Crew Leader	Danial Green
Pilot/s	Grant Hamilton, Tim Haldane, Gabriel Kalotay
System Operator/s	Danial Green
Engineer	Clint Hazelwood
Field Data Processing	Martyn Allen
Office Data Processing	Matthew Lawrence

## 1.4 Area Map



## 2. SURVEY SPECIFICATIONS AND PARAMETERS

### 2.1 Area Co-ordinates

The survey area was located within UTM Zone 53S, Central Meridian = 135  
(Note - Co-ordinates in WGS84 Zone 53)

#### Toro Energy Area

St E	St Nth	End E	End Nth
274941	7463991	274960	7473201
264996	7473102	264996	7460214
255033	7454466	255029	7471058
245004	7469083	245009	7454364
234979	7452286	234969	7468868
225015	7468722	225018	7452084
215001	7451878	214996	7468486
204976	7468385	204965	7451753
194999	7451508	195001	7463136

#### Scimitar Resources Area

St E	St Nth	St E	St Nth
299823	7444851	181703	7444874
194992	7439986	194998	7451440
225018	7452150	225018	7440037
234975	7439984	234980	7452216
234969	7468868	234992	7481796
264993	7491733	264996	7473168
264996	7460214	264995	7440027
255037	7440044	255034	7454536
255029	7471058	255039	7476635
227256	7474969	299465	7475161
244872	7476509	245003	7469150
245009	7454430	245005	7440029
274958	7439845	274941	7463991
274960	7473201	274949	7491622
290085	7491816	290090	7440455

### 2.2 Survey Area Parameters

Job Number	-	1900
Survey Company	-	Fugro Airborne Surveys Pty Ltd
Date Flown	-	18 <sup>th</sup> July 2007
Client	-	Toro Energy Limited & Scimitar Resources Limited
EM System	-	25 Hz TEMPEST
Navigation	-	Real-time differential GPS
Datum	-	GDA94 (Zone 53)
Area Name	-	Southern NT, Northern Territory
Nominal Terrain Clearance	-	120 m
<b>Toro Energy Limited</b>		
Traverse Line Spacing	-	Variable
Traverse Line Direction	-	Variable
Traverse Line Numbers	-	10023 – 10101
Line Kilometres	-	132 km
<b>Scimitar Resources Limited</b>		
Traverse Line Spacing	-	Variable
Traverse Line Direction	-	Variable
Traverse Line Numbers	-	10010 – 10121
Line Kilometres	-	413 km
Total Survey Line Kilometres	-	550 km

### 2.3 Flight Plans

The flight plans are given in Appendix 1.

## **2.4 Job Safety Plan**

A Job Safety Plan was prepared and implemented in accordance with the Fugro Airborne Surveys Occupational Safety & Health Management System.

### 3. AIRCRAFT EQUIPMENT AND SPECIFICATIONS

#### 3.1 Aircraft

Manufacturer	-	CASA
Model	-	C212-200 Turbo Prop
Registration	-	VH-TEM
Ownership	-	Fugro Airborne Surveys Pty Ltd

#### 3.2 TEMPEST System Specifications

Specifications of the TEMPEST Airborne EM System (Lane et al., 2000) are:

• Base frequency	-	25 Hz
• Transmitter area	-	221 m <sup>2</sup>
• Transmitter turns	-	1
• Waveform	-	Square
• Duty cycle	-	50%
• Transmitter pulse width	-	10 ms
• Transmitter off-time	-	10 ms
• Peak current	-	280 A
• Peak moment	-	61880 Am <sup>2</sup>
• Average moment	-	30940 Am <sup>2</sup>
• Sample rate	-	75 kHz on X and Z
• Sample interval	-	13 microseconds
• Samples per half-cycle	-	1500
• System bandwidth	-	25 Hz to 37.5 kHz
• Flying height	-	120 m (subject to safety considerations)
• EM sensor	-	Towed bird with 3 component dB/dt coils
• Tx-Rx horizontal separation	-	120 m (nominal)
• Tx-Rx vertical separation	-	35 m (nominal)
• Stacked data output interval	-	200 ms (~12 m)
• Number of output windows	-	15
• Window centre times	-	13 µs to 16.2 ms
• Magnetometer	-	Stinger-mounted cesium vapour
• Magnetometer compensation	-	Fully digital
• Magnetometer output interval	-	200 ms (~12 m)
• Magnetometer resolution	-	0.001 nT
• Typical noise level	-	0.2 nT
• GPS cycle rate	-	1 second

##### 3.2.1 EM Receiver and Logging Computer

The EM receiver computer is a Picodas PDAS-1000 data acquisition system. The EM receiver computer executes a proprietary program for system control, timing, data acquisition and recording. Control, triggering and timing is provided to the TEMPEST transmitter and DSP signal processing boards by the timing card, which ensures that all waveform generation and sampling is accomplished with high accuracy. The timing card is synchronised to GPS through the use of the PPS output from the system GPS card. Synchronisation is also provided to the magnetometer processor card for the purpose of accurate magnetic sampling with respect to the EM transmitter waveform.

The EM receiver computer displays information on the main screen during system calibrations and survey line acquisition to enable the airborne operator to assess the data quality and performance of the system.

### **3.2.2 TEMPEST Transmitter**

The transmitted waveform is a square wave of alternating polarity, which is triggered directly from the EM receiver computer. The nominal transmitter base frequency was 25 Hz with a pulse width of 10ms (50 % duty cycle). Loop current waveform monitoring is provided by a current transformer located directly in the loop current path to allow for full logging of the waveform shape and amplitude, which is sampled by the EM receiver.

### **3.2.3 TEMPEST 3-Axis Towed Bird Assembly**

The TEMPEST 3-axis towed bird assembly provides accurate low noise sampling of the X (horizontal in line), Y (horizontal transverse) and Z (vertical) components of the electromagnetic field. The receiver coils measure the time rate of change of the magnetic field (dB/dt). Signals from each axis are transferred to the aircraft through a tow cable specifically designed for its electrical and mechanical properties.

## **3.3 PDAS 1000 Survey Computer**

The SURVEY computer is a PICODAS PDAS 1000 data acquisition system. The SURVEY computer executes a proprietary program for acquisition and recording of location, magnetic and ancillary data. Data are presented both numerically and graphically in real time on the VGA LCD display, which provides an on-line display capability. The operator may alter the sensitivity of the displays on-line to assist in quality control. Selected EM data are transferred from the EM receiver computer to the SURVEY computer for QC display.

### **3.3.1 Cesium Vapour Magnetometer Sensor**

A cesium vapour magnetometer sensor is utilised on the aircraft and consists of the sensor head and cable, and the sensor electronics. The sensor head is housed at the end of a composite material tail stinger.

### **3.3.2 Magnetometer Processor Board**

A Picodas magnetometer processor board is used for de-coupling and processing the Larmor frequency output of the magnetometer sensor. The processor board interfaces with the PDAS 1000 survey computer, which initiates data sampling and transfer for precise sample intervals and also with the EM receiver computer to ensure that the magnetic samples remain synchronised with the EM system.

### **3.3.3 Fluxgate Magnetometer**

A tail stinger mounted Bartington MAG-03MC three-axis fluxgate magnetometer is used to provide information on the attitude of the aircraft. This information is used for compensation of the measured magnetic total field.

### **3.3.4 GPS Receiver**

A Novatel GPScard 951R is utilised for airborne positioning and navigation. Satellite range data are recorded for generating post processed differential solutions.

### **3.3.5 Differential GPS Demodulator**

The OMNISTAR differential GPS service provides real time differential corrections.

### 3.4 Navigation System

A Picodas PNAV 2001 Navigation Computer is used for real-time navigation. The PNAV computer loads a pre-programmed flight plan from disk which contains boundary co-ordinates, line start and end co-ordinates, local co-ordinate system parameters, line spacing, and cross track definitions. The WGS-84 latitude and longitude positional data received from the Novatel GPScard contained in the SURVEY computer is transformed to the local co-ordinate system for calculation of the cross track and distance to go values. This information, along with ground heading and ground speed, is displayed to the pilot numerically and graphically on a two line LCD display, and on an analog HSI indicator. It is also presented on a LCD screen in conjunction with a pictorial representation of the survey area, survey lines, and ongoing flight path.

The PNAV is interlocked to the SURVEY computer for auto selection and verification of the line to be flown. The GPS information passed to the PNAV 2001 navigation computer is corrected using the received real time differential data, enabling the aircraft to fly as close to the intended track as possible.

### 3.5 Altimeter System

#### 3.5.1 Radar Altimeter

Model:	Sperry Stars RT-220 radio altimeter system
Sample interval:	0.2 second
Accuracy:	+/- 1.5 % of indicated altitude.

The Sperry radio altimeter is a high quality instrument whose output is factory calibrated. It is fitted with a test function which checks the calibration of a terrain clearance of 100 feet, and altitudes which are multiples of 100 feet. The aircraft radio altitude is recorded onto digital tape as well as displayed on the aircraft chart recorder. The recorded value is the average of the altimeters output during the previous second.

#### 3.5.2 Barometric Altimeter

Output of a Digiquartz 215A-101 pressure transducer is used for calculating the barometric altitude of the aircraft. The atmospheric pressure is taken from a gimbal-mounted probe projecting 0.5 metres from the wing tip of the aircraft and fed to the transducer mounted in the aircraft wingtip.

### 3.6 Video Tracking System

The video tape recorded by a PAL VHS colour video system is synchronised with the geophysical record by a digital fiducial display, which is recorded along with GPS latitude and longitude information and survey line number.

### 3.7 Data Recorded by the Airborne Acquisition Equipment

Raw EM data including fiducial, local time, X, Y, Z axis sensor response, current monitor and bird auxiliary sensor output are recorded on the EM receiver computer as “G” EM files.

The Survey computer records all other survey data including aeromagnetic and GPS data using as “S” Survey files, and “R” Rover files containing GPS raw range data for post processing.

## **4. GROUND DATA ACQUISITION EQUIPMENT AND SPECIFICATIONS**

### **4.1 Magnetic Base Station**

A Scintrex ENVI magnetometer and a CF1 magnetometer were used to measure the daily variations of the Earth's magnetic field. The base stations were established in an area of low gradient, away from cultural influences. The base stations were run continuously throughout the survey flying period with a sampling interval of 5 seconds at a sensitivity of 0.01 nT. The base station data were closely examined after each day's production flying to determine if any data had been acquired during periods of out-of-specification diurnal variation. The base stations were located approximately 80 m apart at Alice Springs Airport.

### **4.2 GPS Base Station**

A GPS base logging station was set up at Alice Springs Airport. The GPS antenna was positioned on the roof of the hanger at Alice Springs Airport.

The GPS base system was comprised of a Novatel GPS PC card mounted in a portable IBM computer. The computer is connected to a mains UPS backup, with a reserve capacity of approximately 100 minutes, to ensure continuous data logging in the event of mains power interruptions.

The GPS base station position was calculated by logging data continuously at the base position over a period of approximately 24 hours. These data were then statistically averaged to obtain the position of the base station using GrafNav software.

The calculated GPS base position was (in WGS84):

Lat: 23° 48' 18.73415" S

Long: 133° 54' 18.47031" E

Height: 552.030 m. (WGS84 Ellipsoidal Height)

## **5. EM AND OTHER CALIBRATIONS AND MONITORING**

At the beginning and end of each individual survey flight, the EM system is checked for background noise levels and performance. All of these checks are conducted at a nominal terrain clearance of 600 m (2000 ft) to eliminate ground response.

These checks include:-

### **5.1 Pre-Flight Barometer Calibration: Line C1511**

A recording of the barometer output at a known elevation is carried out before take-off to assist with calibration and determination of drift during the flight. The barometer is used as a back-up to the GPS for aircraft altitude.

### **5.2 Pre-Flight Zero: Line C9001**

This manoeuvre is performed once the aircraft is established en route to the survey area. Background EM levels are recorded and assessed by the airborne operator to determine if:-

- a. the system noise level is acceptable,
- b. the response had not varied significantly from previous flights, and
- c. the spheric level is acceptable.

These data are recorded for approximately 90 seconds.

### **5.3 Pre-Flight Swoops: Line C9002**

This manoeuvre is conducted immediately after the pre sortie zero. During this manoeuvre the relative position of the towed sensor is deliberately made to vary relative to the aircraft. The EM data are monitored by the airborne operator to confirm correct operation of the system during the manoeuvre.

### **5.4 Post-Flight Zero: Line C9003**

This calibration is performed immediately following the completion of the survey sorties. Background EM levels are recorded to characterise any changes occurred in the system over the duration of the flight. These data are recorded for approximately 90 seconds.

### **5.5 Post-Flight Barometer Calibration: Line C1611**

A recording of the barometer output is repeated following landing at the end of the flight to assist with calibration and determination of drift during the flight.

### **5.6 Additive EM Measurements: Lines C9004, C9005, and C9007**

A recording of the background signal through the X, Y and Z receiver coil inputs is carried out before and/or after acquisition of data for survey lines on each flight. These measurements may be made with the transmitter on (C9004, C9005) or with the transmitter off (C9007). The signal from the receiver coils is removed from the signal pathway by disconnecting the power to the bird at the winch inside the aircraft.

### **5.7 Dynamic Magnetometer Compensation**

To limit aircraft manoeuvre effects on the magnetic data that can be of the same spatial wavelength as the signals from geological sources, compensation calibration lines are flown in a low magnetic gradient area close to the survey. This involves flying a series of tests on the survey line heading and approximately 15 degrees either side to accommodate small heading variations whilst flying survey lines. The data for each heading consists of a series of aircraft manoeuvres, including pitches, rolls and yaws. This is done to artificially create the most extreme possible attitude the aircraft may encounter whilst on

survey. Data from these lines are used to derive compensation coefficients for removing magnetic noise induced by the aircraft's attitude in the naturally occurring magnetic field.

Compensation data were acquired on the 18<sup>th</sup> of July 2007.

### 5.8 Parallax Checks

Due to the relative positions of the EM towed bird and the magnetometer instruments on the aircraft and to processing / recording time lags, raw readings from each vary in position. To correct for this and to align selected anomaly features on lines flown in opposite directions, magnetics, EM data and the altimeters are 'parallaxed' with respect to the position information. System parallax is checked occasionally or following any major changes in the aircraft system which are likely to affect the parallax values.

Variable	Parallax Value
Magnetics	0.6 s
GPS	0 s
Radar Altimeter	0.6 s
EM – X	0.2 s
EM – Z	1.4 s

### 5.9 Radar Altimeter Calibration

The radar altimeter is checked for accuracy and linearity every 12 months or when any change in a key system component requires this procedure to be carried out. This calibration allows the radar altimeter data to be compared and assessed with other height data (GPS and barometric) to confirm the accuracy of the radar altimeter over its operating range.

Absolute radar and barometric altimeter calibration was carried out over water at Mandurah, WA and was successful in calibrating the radar altimeter to information provided by the GPS and barometer instrument. Calibration factors were as expected. The calibration procedure also provides parallax information required for positional correction of the radar and GPS altimeters.

### 5.10 Heading Error Checks

Historically, heading error checks have been part of the aeromagnetic data acquisition procedure but they are no longer used. Fugro Airborne Surveys now calculates these effects using the aircraft magnetic compensation system and specially developed software. The precision to which these effects are now calculated and corrected for is far in excess of the manual methods used in the past.

## 6. DATA PROCESSING

### 6.1 Field Data Processing

#### 6.1.1 Quality Control Specifications

##### 6.1.1.1 Navigation Tolerance

The re-flight specifications applied for the duration of the survey were:

Electronic Navigation - absence of electronic navigation data (e.g. GPS base station fails).

Flight Path – flight path deviates from the flight plan by more than 50% of the nominal line spacing for more than 5 km or where lines cross.

Altitude - terrain clearance continuously exceeds the nominal terrain clearance by plus or minus 30 m over a distance of 5 km or more unless to do so would, in the sole opinion of the pilot, jeopardise the safety of the aircraft or the crew or the equipment or would be in contravention of the Civil Aviation Safety Authority regulation such as those pertaining to built up areas.

##### 6.1.1.2 Magnetism Noise And Diurnal Tolerance

The re-flight specifications applied for the duration of the survey were:

Magnetic Diurnal - where the magnetometer base station data exceeds a 10 nT change in 10 minutes.

##### 6.1.1.3 Electromagnetic Data

The quality control checks on the electromagnetic data were:

Noise - where RMS noise in the last channel of the EM data exceeds 0.1 fT over 3 km for B-field (assessed in a resistive region) or where FAS believes an important anomaly is rendered un-interpretable.

Sferics – where sferic activity renders a potential anomaly un-interpretable.

### 6.1.2 In-Field Data Processing

Following acquisition, multiple copies of the EM data are made onto DVDs or CDs. The EM, location, magnetic and ancillary data are then processed at the field base to the point that the quality of the data from each flight can be fully assessed. Copies of the raw and processed data are then transferred to Perth for final data processing. A more comprehensive statement of EM data processing is given in section 6.2.3.

## 6.2 Final Data Processing

### 6.2.1 Magnetism

Magnetic data were compensated for aircraft manoeuvre noise using coefficients derived from the appropriate compensation flight. Base station data is edited so that all significant spikes, level shifts and null data are eliminated.

A diurnal base value was then added.

Area	Base Value
Southern NT	53325 nT

A lag was applied to synchronise the magnetic data with the navigation data.

The International Geomagnetic Reference Field (IGRF) 2005 model (updated for secular variation 2007.5) was removed from the levelled total field magnetics. An IGRF base value was then added to the data.

Area	Base Value
Southern NT	52942 nT

## 6.2.2 Derived Topography

Aircraft navigation whilst in survey mode is via real time differential GPS, obtained by combining broadcast differential corrections with on-board GPS measurements. Terrain clearance is measured with a radar altimeter.

The ground elevation, relative to the WGS84 spheroid used by GPS receiver units, is obtained by subtracting the terrain clearance from the aircraft altitude, noting the vertical separation between the GPS antenna and the radar altimeter, and applying suitable parallax corrections between the two measurements.

The digital elevation model derived from this survey can be expected to have an absolute accuracy of +/- several metres in areas of low to moderate topographic relief. Sources of error include uncertainty in the location of the GPS base station, variations in the radar altimeter characteristics over ground of varying surface texture, and the finite footprint of the radar altimeter.

An N-Value is subtracted to correct the final data to the Australian Height Datum (AHD).

---

The accuracy of the elevation calculation is directly dependent on the accuracy of the two input parameters, radar altitude and GPS altitude. The radar altitude value may be erroneous in areas of heavy tree cover, where the altimeter reflects the distance to the tree canopy rather than the ground. The GPS altitude value is primarily dependent on the number of available satellites. Although post-processing of GPS data will yield X and Y accuracies in the order of 1-2 metres, the accuracy of the altitude value is usually much less, sometimes in the  $\pm 5$  metre range. Further inaccuracies may be introduced during the interpolation and gridding process.

Because of the inherent inaccuracies of this method, no guarantee is made or implied that the information displayed is a true representation of the height above sea level. Although this product may be of some use as a general reference, **THIS PRODUCT MUST NOT BE USED FOR NAVIGATION PURPOSES.**

---

### 6.2.3 Electromagnetic Data Processing

Details of the pre-processing applied to TEMPEST data can be found in Lane et al. (2000).

#### 6.2.3.1 Standard EM Processing

##### Calibration

High altitude calibration data are used to characterise the system response in the absence of any ground response.

##### Cleaning and Stacking

Routines to suppress sferic noise, powerline noise, VLF noise, coil motion noise (collectively termed “cleaning”) and to stack the data are applied to the survey line data. Output from the stacking filter is drawn at 0.2 second intervals. The stacked data are saved to file as an internal data management practice.

##### Deconvolution and Binning

The survey height stacked data are deconvolved using the high altitude reference waveform. The effect of currents in the transmitter loop and airframe (“primary”) are then removed, leaving a “pure” ground response. The deconvolved ground response data are then transformed to B-field response for a perfect 100% duty cycle square wave. Finally, the evenly spaced samples are binned into a number of windows.

**Table of TEMPEST window information for 25Hz base frequency**

Window #	Start sample	End sample	No samples	of start time (s)	End time (s)	centre time (s)	centre time (ms)
1	1	2	2	0.000007	0.000020	0.000013	0.013
2	3	4	2	0.000033	0.000047	0.000040	0.040
3	5	6	2	0.000060	0.000073	0.000067	0.067
4	7	10	4	0.000087	0.000127	0.000107	0.107
5	11	16	6	0.000140	0.000207	0.000173	0.173
6	17	26	10	0.000220	0.000340	0.000280	0.280
7	27	42	16	0.000353	0.000553	0.000453	0.453
8	43	66	24	0.000567	0.000873	0.000720	0.720
9	67	102	36	0.000887	0.001353	0.001120	1.120
10	103	158	56	0.001367	0.002100	0.001733	1.733
11	159	246	88	0.002113	0.003273	0.002693	2.693
12	247	384	138	0.003287	0.005113	0.004200	4.200
13	385	600	216	0.005127	0.007993	0.006560	6.560
14	601	930	330	0.008007	0.012393	0.010200	10.200
15	931	1500	570	0.012407	0.019993	0.016200	16.200

The data are reviewed after windowing. Any decisions involving re-flights due to AEM factors are made at this point.

##### Raw and Final EM Data

The “raw” or “uncorrected” EM amplitudes reflect, not only the variations in ground conductivity, but the variations in geometry of the various parts of the EM measurements (i.e. transmitter loop pitch, transmitter loop roll, transmitter loop terrain clearance, transmitter loop to receiver coil horizontal longitudinal separation, transmitter loop to receiver coil horizontal transverse separation, and transmitter loop to receiver coil vertical separation) during the survey. For example, the largest influence on the early time EM amplitude is the terrain clearance of the transmitter loop. The larger the terrain clearance, the smaller the amplitude. Later window times (larger window number) show diminished variations due to terrain clearance.

“Final” or “geometry-corrected” located data are produced for optimum presentation of the EM amplitude data in image format (e.g. window amplitude images, principal component analysis images derived from the window amplitudes (Green, 1998b)). Between “raw” and “final” states, the ground response data undergo an approximate correction to produce data from a nominated standard geometry. A dipole-image method (Green, 1998a) is used to adjust the data to the response that would be expected at a standard terrain clearance (120m), standard transmitter loop pitch and roll (zero degrees), and a standard transmitter loop to receiver coil geometry (120m behind and 35 below the aircraft). These variables have been set to their respective standard values in the “final” located data (whereas the “raw” located data file contains the variable field data). Zero parallax is applied to transmitter loop pitch, roll, terrain clearance, X component EM and Z component EM data prior to geometry correction. Over extremely conductive ground (e.g. > 100 S conductance), the estimates for transmitter loop to receiver coil separation determined from the primary field coupling factors may be in error at the metre scale due to uncertainty in the estimation of the primary field. This will influence the accuracy of very early time window amplitude information in the “geometry-corrected” located data. Receiver coil pitch has a significant effect on early time Z component response and late time X component response (Green and Lin, 1996). Receiver coil roll impacts early time Z component response.

### **Levelling**

Limited range micro-levelling may be applied to the final window amplitudes for presentation purposes, principally for multi-flight surveys or when isolated re-flight lines are present.

### **6.2.3.2 Factors and Corrections**

#### **Geometric Factor**

The geometric factor gives the ratio of the strength of the primary field coupling between the transmitter loop and the receiver coil at each observation relative to the coupling observed at high altitude during acquisition of reference waveform data. Variations in this factor indicate a change in the attitude and/or relative separation of the transmitter loop and the receiver coil.

#### **Transmitter-Receiver Geometry**

Transmitter to receiver geometry values for each observation are derived from the high altitude reference waveforms and knowledge of the system characteristics. These data are available in the located data (see section 6.2.6.1 for “standardised” values)

#### **GPS Antenna, Laser Altimeter and Transmitter Loop Offset Corrections**

The transmitter loop was mounted 0.1m above the GPS antenna on the aircraft. The GPS antenna is 2.3m above the belly of the aircraft. The laser altimeter sensor is mounted in the belly of the aircraft. Therefore a total of 2.4m (0.1m + 2.3m) was added to the laser altimeter data to determine the transmitter loop height above the ground.

#### **Transmitter Loop Pitch and Roll Correction**

Measured vertical gyro aircraft pitch and roll attitude measurements are converted to transmitter loop pitch and roll by adding -0.9 degrees for pitch and -0.1 degrees for roll. Nose up is positive for pitch, and left wing up is positive for roll.

### **6.2.3.3 Primary Sources of EM Noise**

A number of “monitor” values are calculated during processing to assist with interpretation. They generally represent quantities that have been removed as far as is practical from the data, but may still be present in trace amounts. These are more significant for interpretation of discrete conductors than for general mapping applications.

#### **Sferic Monitor**

Sferics are the electromagnetic signals associated with lightning activity. These signals travel large distances around the Earth. Background levels of sferics are recorded at all times from lightning activity in tropical areas of the world (eg tropical parts of Asia, South America and Africa). Additional higher amplitude signals are produced by “local” lightning activity (ie at distances of kilometres to hundreds of kilometres).

The sferic monitor is the sum of the absolute differences brought about by the sferic filter operations, summed over 0.2 second intervals, normalised by the receiver effective area. It is given in units of  $\mu\text{V}/\text{sq.m}/0.2\text{s}$ . Many sferics have a characteristic form that is well illustrated by figure 2 in Garner and Thiel (2000). The high frequency, initial part of a sferic event can be detected and filtered more easily than the later, low frequency portion. The sferic monitor indicates where at least the high frequency portion of a sferic has been successfully removed, but it is quite possible that lower frequency elements of the sferic event may have eluded detection, passing through to the window amplitude data. Thus, discrete anomalies coincident with sferic activity as indicated by the sferic monitor should be down-weighted relative to features clear of any sign of sferic activity.

### **Low Frequency Monitor**

The Low Frequency Monitor (LFM) makes use of amplitudes at frequencies below the base frequency which are present in the streamed data to estimate the amplitude of coil motion (Earth magnetic field) noise at the base frequency in  $\log_{10}(\text{pV}/\sqrt{\text{Hz}}/\text{sq.m})$ . The coil motion noise below the base frequency is rejected through the use of tapered stacking, but the coil motion noise at the base frequency itself is not easily removed. A sharp spike in the LFM can be an indicator of a coil motion event (eg the bird passing through extremely turbulent air). Note that the LFM will also respond to sferic events with an appreciable low frequency (sub-base frequency) component. This situation can be inferred when both the LFM and sferic monitors show a discrete kick.

### **Powerline Monitor**

The powerline monitor gives the amplitude of the received signal at the powerline frequency (50 or 60 Hz) in  $\log_{10}(\text{pV}/\sqrt{\text{Hz}}/\text{sq.m})$ . Careful selection of the base frequency (such that the powerline frequency is an even harmonic of the base frequency) and tapered stacking combine to strongly attenuate powerline signals. When passing directly over a powerline, the rapid lateral variations in the strength and direction of the magnetic fields associated with the powerline can result in imperfect cancellation of the powerline response during stacking. Some powerline-related interference can manifest itself in a form that is similar to the response of a discrete conductor. The exact form of the monitor profile over a powerline depends on the line direction, powerline direction, powerline current, and receiver component, but the monitor will show a general increase in amplitude approaching the powerline.

Grids (or images) of the powerline monitor reveal the location of the transmission lines. Note that the X component (horizontal receiver coil axis parallel with the flight line direction) does not register any response from powerlines parallel to the flight line direction since the magnetic fields associated with powerlines only vary in a direction perpendicular to the powerline. Note also that the Z component (vertical receiver coil axis) shows a narrow low directly over the powerline where the magnetic fields are purely horizontal.

### **Very Low Frequency Monitors**

Wide area VLF communication signals in the 15 to 25 kHz frequency band are monitored by the TEMPEST system. In the Australian region, signals at 18.2 kHz, 19.8 kHz, 21.4 kHz and 22.2 kHz are monitored as the amplitude of the received signal at these frequencies in  $\log_{10}(\text{pV}/\sqrt{\text{Hz}}/\text{sq.m})$ . The strongest signal comes from North West Cape (19.8 kHz). The signal at 18.2 kHz is often observed to pulse in a regular sequence. These strong narrow band signals have some impact on the high frequency response of the system, but they are strongly attenuated by selection of the base frequency and tapered stacking. The VLF transmissions are strongest in amplitude, in the horizontal direction at right angles to the direction to the VLF transmitter. This directional dependence enables the VLF monitors to be used to indicate the receiver coil attitude.

#### **6.2.3.4 Other Sources of EM Noise**

##### **Man-made periodic discharges**

If an image of the Z component sferic monitor shows the presence of spatially coherent events, then pulsed cultural interference would be strongly suspected. Since sferic signals are much stronger in the horizontal plane than in the vertical plane, few sferics of significant amplitude are recorded in Z component data. In contrast, evidence of cultural interference is generally swamped by true sferics in X component sferic monitor images.

Electric fences are the most common source of pulsed cultural interference. Periodic discharges (eg every second or so) into a large wire loop (fence) produce very large spikes in raw data. These are attenuated to a large degree by the sferic filter, but a residual artefact can still be present in the processed data.

### Coil motion / Earth field noise

A change in coupling between the receiver coil and the ambient magnetic field will induce a voltage in the receiver coil. This noise is referred to as coil motion or Earth field noise. Receiver coils in the towed bird are suspended in a fashion that attempts to keep this noise below the noise floor at frequencies equal to and above the base frequency of the system. Severe turbulence, however, can result in 'coil knock events' that introduce noise into the processed data.

### Grounded metal objects

Grounded extensive metal objects such as pipelines and rail lines can qualify as conductors and may produce a response that is visible in processed data. Grounded metal objects produce a response similar to shallow, highly conductive, steeply dipping conductors. These objects can sometimes be identified from good quality topographic maps, from aerial photographs, by viewing the tracking video, from their unusual spatial distribution (ie often a series of linear segments) and in some circumstances from their effect on the powerline monitor. A powerline running close to a long metal object will induce a 50 Hz response in the object.

## 6.2.4 Conductivity Depth Images (CDI)

CDI conductivity sections for TEMPEST data were calculated using EMFlow and then modified to reflect the finite depth of investigation using an in-house routine, *Sigtime*.

The *Sigtime* routine removes many of the spurious conductive features that appear at depth as a result of fitting long time constant exponential decays to very small amplitude features in the late times. For each observation, the time when the response falls below a signal threshold amplitude is determined. This time is transformed into a diffusion depth with reference to the conductivity values determined for that observation. Anomalous conductivity values below this depth are replaced by background values or set to undefined, reflecting the uncertainty in their origin. The settings and options applied are indicated in the appropriate header files for *Sigtime* output. This procedure is different to that which would be obtained by filtering conductivity values using either a constant time or constant depth across the entire line.

The "final" data for each area were input into version 5.10 of EMFlow to calculate Conductivity Depth Images (CDI). Conductivity values were calculated at each point then run through *Sigtime*. This processing was completed for the X component data.

EMFlow was developed within the CRC-AMET through AMIRA research projects (Macnae et al, 1998, Macnae and Zonghou, 1998, Stolz and Macnae, 1998). The software has been commercialised by Encom Technology Pty Ltd. Examples of TEMPEST conductivity data can be seen in Lane et al. (2000), Lane et al. (1999), and Lane and Pracillio (2000).

Conductivity values were calculated to a depth of 200m below surface at each point, using a depth increment of 2m and a conductivity range of 1-2000mS/m.

## 6.2.5 System Specifications for Modelling TEMPEST Data

Differences between the specifications for the acquisition system, and those of the virtual system for which processed results are given, must be kept in mind when forward modelling, transforming or inverting TEMPEST data.

Acquisition is carried out with a 50% duty cycle square transmitter current waveform and dB/dt sensors.

During processing, TEMPEST EM data are transformed to the response that would be obtained with a B-field sensor for a 100% duty cycle square waveform at the base frequency, involving a 1A change in current (from -0.5A to +0.5A to -0.5A) in a 1sq.m transmitter. Data are given in units of femtotesla (fT =  $10^{-15}$  Tesla). It is this configuration, rather than the actual acquisition configuration, which must be specified when modelling TEMPEST data.

Window timing information is given above (see section 6.2.3).

### 6.2.5.1

### 6.2.5.2 Standard Height and Geometry

The “final” EM data have been standardised through an approximate transformation to a standard transmitter loop terrain clearance, transmitter loop pitch and roll of zero degrees, and a fixed transmitter loop to receiver coil geometry (roughly equal to the average “raw” geometry values). Transmitter loop pitch, transmitter loop roll and transmitter loop terrain clearance values for each observation have been modified to reflect the standard values. Hence, the “final” (fixed) geometry values should be used if modelling with the final X- and Z-component amplitude data - the following table summarises the values used to correct the transmitter height/pitch/roll/geometry to.

**Table of values used to standardise transmitter loop height, pitch, roll and geometry**

Variable	Standardised value
Transmitter loop pitch	0 degrees
Transmitter loop roll	0 degrees
Transmitter loop terrain clearance	120 metres
Transmitter loop – to – receiver coil geometry	120 metres behind and 35 metres below the aircraft

### 6.2.5.3 Parallax

The located data files utilise the following parallax values :-

- magnetics = 0.6 fiducials (3 observations from the zero parallax position),
- radar altimeter = 0.6 fiducials (3 observations from the zero parallax position),
- EM X-component = 0.2 fiducials (1 observation from the zero parallax position),
- EM Z-component = 1.4 fiducials (7 observations from the zero parallax position),

These EM parallax values are optimised for aligning the EM response amplitudes for horizontal or broad steeply dipping conductors, which account for the majority of responses in regolith-dominated terrains such as this.

For optimum gridded display of the response for discrete vertical or narrow conductors, the following EM parallax values are appropriate :-

- EM X-component = 1.8 fiducials (9 observations from the zero parallax position, or 8 observations from the “horizontal” parallax position),
- EM Z-component = 0.6 fiducials (3 observations from the zero parallax position, or -4 observations from the “horizontal” parallax position).

(NB Positive parallax values are defined in this case as shifting the indicated quantity back along line to smaller fiducial values. Location information remains in the zero parallax state.)

### 6.2.6 Delivered Products

Appendix V contains a complete list of all data supplied digitally.

Digital located data in ASCII and Geosoft GDB format was produced, containing the raw and final, X and Z EM data as well as magnetics and digital elevation. The header file can be found in Appendix IV.

A list of gridded and map products can be found in Appendix V.

Acquisition and processing report in hardcopy and digital format.

## **7. REFERENCES**

- Garner, S.J., Thiel, D.V., 2000, Broadband (ULF-VLF) surface impedance measurements using MIMDAS: Exploration Geophysics, 31, 173-178.
- Green, A., 1998. Altitude correction of time domain AEM data for image display and geological mapping, using the Apparent Dipole Depth (ADD) method. Expl. Geoph. 29, 87-91.
- Green, A., 1998. The use of multivariate statistical techniques for the analysis and display of AEM data. Expl. Geoph. 29, 77-82.
- Green, A., Lin, Z., 1996. Effect of uncertain or changing system geometry on airborne transient electromagnetic data: CSIRO Expl. and Mining Research News No. 6, August 1996, 9-11, CSIRO Division of Exploration and Mining.
- Lane, R., 2000, Conductive unit parameters : summarising complex conductivity distributions: Paper accepted for presentation at the SEG Annual Meeting, August 2000.
- Lane, R., Green, A., Golding, C., Owers, M., Pik, P., Plunkett, C., Sattel, D., Thorn, B., 2000, An example of 3D conductivity mapping using the TEMPEST airborne electromagnetic system: Exploration Geophysics, 31, 162-172.
- Lane, R., Leeming, P., Owers, M., Triggs, D., 1999, Undercover assignment for TEMPEST: Preview, Issue 82, 17-21.
- Lane, R., Pracilio, G., 2000: Visualisation of sub-surface conductivity derived from airborne EM, SAGEEP 2000, 101-111.

## SOUTHERN NT

```

JOB_Number      1900
CLIENT          Scimitar and Toro Resources
AREA_NAME       1
PLANNED_BY      MRA
|
SPHEROID        22  W.G.S_1984  6378137.0  298.257223563  0.9996
DELTAXYZ        0.0  0.0  0.0  0.0  0.0  0.0  0.0
HEMISPHERE       SOUTH
UTM_ORIGIN       53      135      135
BOUNDARY         1      180424      7492626  -22.643295  +131.890817  -223835.9  +1315326.9  12
BOUNDARY         2      300450      7492626  -22.661698  +133.057890  -223942.1  +1330328.4  12
BOUNDARY         3      300450      7439007  -23.145788  +133.050982  -230844.8  +1330303.5  12
BOUNDARY         4      180424      7439007  -23.126947  +131.879771  -230737.0  +1315247.2  12
SQUARE_KMS      6435.674
|
NAVTYPE          NOVATEL
NAVMODE          U.T.M
PLAN_TYPE        Normal
LINE_TYPE        S.LINE      X.LINE      0      0
HEADING          0      90
SPACING          250      1000      250      250
OVER_LINE        1      1
OVERFLY          0      0
MIN_LENGTH       2      2
FIRST_LINE       10      10
INCREMENT        1      1
X_TRACK          100      100
MASTER_PT        1      180424      7492626  -22.643295  +131.890817
MASTER_NEW       0  Not implemented.
KM_IN_AREA       547      0
KM+OVERFLY       547      0

```

## APPENDIX II – Weekly Acquisition Reports

[illegible]

**Toro Energy Limited**

COMM

COMM

COMM Total Kilometres : 131.50

## COMM

COMM

COMM Total Kilometres : 413.57

## APPENDIX IV – Located Data Format

### Header for final data file

#### TORO ENERGY LIMITED

```

COMM JOB NUMBER: 1900
COMM AREA NUMBER: 1
COMM SURVEY COMPANY: Fugro Airborne Surveys
COMM CLIENT: Toro Energy Limited
COMM SURVEY TYPE: 25Hz TEMPEST Survey
COMM AREA NAME: Southern NT
COMM STATE: NT
COMM COUNTRY: Australia
COMM SURVEY FLOWN: July, 2007
COMM LOCATED DATA CREATED: Aug 2007
COMM
COMM DATUM: GDA94
COMM PROJECTION: MGA
COMM ZONE: 53
COMM
COMM SURVEY SPECIFICATIONS
COMM
COMM TRAVERSE LINE SPACING: variable
COMM TRAVERSE LINE DIRECTION: variable
COMM TIE LINE SPACING: n/a
COMM TIE LINE DIRECTION: n/a
COMM NOMINAL TERRAIN CLEARANCE: 120 m
COMM FINAL LINE KILOMETRES: 132 km
COMM
COMM LINE NUMBERING
COMM
COMM TRAVERSE LINE NUMBERS: 10023 - 10101
COMM TIE LINE NUMBERS: n/a
COMM
COMM SURVEY EQUIPMENT
COMM
COMM AIRCRAFT: CASA C212 Turbo Prop, TEM
COMM
COMM MAGNETOMETER: Scintrex Cs-2 Cesium Vapour
COMM INSTALLATION: stinger mount
COMM RESOLUTION: 0.001 nT
COMM RECORDING INTERVAL: 0.2 s
COMM
COMM ELECTROMAGNETIC SYSTEM: 25Hz TEMPEST
COMM INSTALLATION: Transmitter loop mounted on the aircraft
COMM Receiver coils in a towed bird
COMM COIL ORIENTATION: X,Z
COMM RECORDING INTERVAL: 0.2 s
COMM SYSTEM GEOMETRY:
COMM RECEIVER DISTANCE BEHIND THE TRANSMITTER: -120 m
COMM RECEIVER DISTANCE BELOW THE TRANSMITTER: -35 m
COMM
COMM RADAR ALTIMETER: Sperry RT-220
COMM RECORDING INTERVAL: 0.2 s
COMM
COMM NAVIGATION: real-time differential GPS
COMM RECORDING INTERVAL: 1.0 s
COMM
COMM ACQUISITION SYSTEM: PDAS-1000
COMM
COMM DATA PROCESSING
COMM

```

```

COMM MAGNETIC DATA
COMM DIURNAL BASE VALUE APPLIED 53325 nT
COMM PARALLAX CORRECTION APPLIED 0.6 s
COMM IGRF BASE VALUE APPLIED 52942 nT
COMM IGRF MODEL 2005 EXTRAPOLATED TO 2007.5
COMM
COMM ELECTROMAGNETIC DATA
COMM SYSTEM PARALLAX REMOVED, AS FOLLOWS
COMM X-COMPONENT EM DATA 0.2 s
COMM Z-COMPONENT EM DATA 1.4 s
COMM DATA CORRECTED FOR TRANSMITTER HEIGHT, PITCH AND ROLL
COMM DATA CORRECTED FOR TRANSMITTER-RECEIVER GEOMETRY VARIATIONS
COMM CONDUCTIVITY DEPTH INVERSION CALCULATED EMFlow V5.10
COMM CONDUCTIVITIES CALCULATED USING corrected EM DATA
COMM
COMM DIGITAL TERRAIN DATA
COMM PARALLAX CORRECTION APPLIED TO RADAR ALIMETER DATA 0.6 s
COMM PARALLAX CORRECTION APPLIED TO GPS ALIMETER DATA 0.0 s
COMM DTM CALCULATED [DTM = GPS ALTITUDE - RADAR ALTITUDE]
COMM -----
COMM The accuracy of the elevation calculation is directly dependent on
COMM the accuracy of the two input parameters, radar altitude and GPS
COMM altitude. The radar altitude value may be erroneous in areas of heavy
COMM tree cover, where the altimeter reflects the distance to the tree
COMM canopy rather than the ground. The GPS altitude value is primarily
COMM dependent on the number of available satellites. Although
COMM post-processing of GPS data will yield X and Y accuracies in the
COMM order of 1-2 metres, the accuracy of the altitude value is usually
COMM much less, sometimes in the ±5 metre range. Further inaccuracies
COMM may be introduced during the interpolation and gridding process.
COMM Because of the inherent inaccuracies of this method, no guarantee is
COMM made or implied that the information displayed is a true
COMM representation of the height above sea level. Although this product
COMM may be of some use as a general reference,
COMM THIS PRODUCT MUST NOT BE USED FOR NAVIGATION PURPOSES.
COMM -----
COMM
COMM ELECTROMAGNETIC SYSTEM
COMM
COMM TEMPEST IS A TIME-DOMAIN SQUARE-WAVE SYSTEM,
COMM TRANSMITTING AT A BASE FREQUENCY OF 25Hz,
COMM WITH 2 ORTHOGONAL-AXIS RECEIVER COILS IN A TOWED BIRD.
COMM FINAL EM OUTPUT IS RECORDED 5 TIMES PER SECOND.
COMM THE TIMES (IN MILLISECONDS) FOR THE 15 WINDOWS ARE:
COMM
COMM WINDOW START END CENTRE
COMM 1 0.007 0.020 0.013
COMM 2 0.033 0.047 0.040
COMM 3 0.060 0.073 0.067
COMM 4 0.087 0.127 0.107
COMM 5 0.140 0.207 0.173
COMM 6 0.220 0.340 0.280
COMM 7 0.353 0.553 0.453
COMM 8 0.567 0.873 0.720
COMM 9 0.887 1.353 1.120
COMM 10 1.367 2.100 1.733
COMM 11 2.113 3.273 2.693
COMM 12 3.287 5.113 4.200
COMM 13 5.127 7.993 6.560
COMM 14 8.007 12.393 10.200
COMM 15 12.407 19.993 16.200
COMM
COMM PULSE WIDTH: 10 ms
COMM

```

COMM TEMPEST EM data are transformed to the response that would be  
 COMM obtained with a B-field sensor for a 100% duty cycle square  
 COMM waveform at the base frequency, involving a 1A change in  
 COMM current (from -0.5A to +0.5A to -0.5A) in a 1sq.m transmitter.  
 COMM It is this configuration, rather than the actual acquisition  
 COMM configuration, which must be specified when modelling TEMPEST data.  
 COMM

## LOCATED DATA FORMAT

Output field format : DOS - Flat ascii  
 Number of fields : 198

Field	Channel	Description	Units	Undefined
Format				
----	-----	-----	-----	-----
1	LINE	Line		-9999999 i6
2	FLIGHT	Flight		-9999999 i4
3	FID	Fiducial	(s)	-9999999 f8.1
4	LATITUDE	Latitude GDA94	(deg)	-9999999 f13.6
5	LONGITUDE	Longitude GDA94	(deg)	-9999999 f13.6
6	EASTING	Easting MGA53	(m)	-9999999 f11.2
7	NORTHING	Northing MGA53	(m)	-9999999 f12.2
8	TxHeight	GPS height	(m)	-9999999 f8.2
9	Baro	Barometric Altitude	(m)	-9999999 f8.2
10	TxRalt_raw	Raw Radar Altimeter	(m)	-9999999 f8.2
11	TxRalt_final	Final Radar Altimeter	(m)	-9999999 f8.2
12	DTM	DTM	(m)	-9999999 f8.2
13	MAG	Compensated TMI	(nT)	-9999999 f10.3
14	MAG_1VD	Levelled TMI 1VD	(nT/m)	-9999999 f12.5
15	Pitch_Raw	Raw Tx loop pitch	(deg)	-9999999 f10.5
16	Roll_Raw	Raw Tx loop roll	(deg)	-9999999 f10.5
17	HSep_Raw	Raw Tx-Rx horizontal separation	(m)	-9999999 f8.2
18	VSep_Raw	Raw Tx-Rx vertical separation	(m)	-9999999 f8.2
19	Pitch_Final	Final Tx loop pitch	(deg)	-9999999 f10.5
20	Roll_Final	Final Tx loop roll	(deg)	-9999999 f10.5
21	HSep_Final	Final Tx-Rx horizontal separation	(m)	-9999999 f8.2
22	VSep_Final	Final Tx-Rx vertical separation	(m)	-9999999 f8.2
23	EMX_Raw[1]	Raw EMX01 Window	(fT)	-9999999 f12.6
24	EMX_Raw[2]	Raw EMX02 Window	(fT)	-9999999 f12.6
25	EMX_Raw[3]	Raw EMX03 Window	(fT)	-9999999 f12.6
26	EMX_Raw[4]	Raw EMX04 Window	(fT)	-9999999 f12.6
27	EMX_Raw[5]	Raw EMX05 Window	(fT)	-9999999 f12.6
28	EMX_Raw[6]	Raw EMX06 Window	(fT)	-9999999 f12.6
29	EMX_Raw[7]	Raw EMX07 Window	(fT)	-9999999 f12.6
30	EMX_Raw[8]	Raw EMX08 Window	(fT)	-9999999 f12.6
31	EMX_Raw[9]	Raw EMX09 Window	(fT)	-9999999 f12.6
32	EMX_Raw[10]	Raw EMX10 Window	(fT)	-9999999 f12.6
33	EMX_Raw[11]	Raw EMX11 Window	(fT)	-9999999 f12.6
34	EMX_Raw[12]	Raw EMX12 Window	(fT)	-9999999 f12.6
35	EMX_Raw[13]	Raw EMX13 Window	(fT)	-9999999 f12.6
36	EMX_Raw[14]	Raw EMX14 Window	(fT)	-9999999 f12.6
37	EMX_Raw[15]	Raw EMX15 Window	(fT)	-9999999 f12.6
38	EMX_Final[1]	Final EMX01 Window	(fT)	-9999999 f12.6
39	EMX_Final[2]	Final EMX02 Window	(fT)	-9999999 f12.6
40	EMX_Final[3]	Final EMX03 Window	(fT)	-9999999 f12.6
41	EMX_Final[4]	Final EMX04 Window	(fT)	-9999999 f12.6
42	EMX_Final[5]	Final EMX05 Window	(fT)	-9999999 f12.6
43	EMX_Final[6]	Final EMX06 Window	(fT)	-9999999 f12.6
44	EMX_Final[7]	Final EMX07 Window	(fT)	-9999999 f12.6
45	EMX_Final[8]	Final EMX08 Window	(fT)	-9999999 f12.6
46	EMX_Final[9]	Final EMX09 Window	(fT)	-9999999 f12.6
47	EMX_Final[10]	Final EMX10 Window	(fT)	-9999999 f12.6

48	EMX_Final[11]	Final EMX11 Window		(fT)	-9999999	f12.6
49	EMX_Final[12]	Final EMX12 Window		(fT)	-9999999	f12.6
50	EMX_Final[13]	Final EMX13 Window		(fT)	-9999999	f12.6
51	EMX_Final[14]	Final EMX14 Window		(fT)	-9999999	f12.6
52	EMX_Final[15]	Final EMX15 Window		(fT)	-9999999	f12.6
53	X_Sferics	X_Sferics			-9999999	f10.3
54	X_Lowfreq	X_Lowfreq			-9999999	f10.3
55	X_Powerline	X_Powerline			-9999999	f10.3
56	X_VLF1	X_18.2kHz			-9999999	f10.3
57	X_VLF2	X_19.8kHz			-9999999	f10.3
58	X_VLF3	X_21.4kHz			-9999999	f10.3
59	X_VLF4	X_22.2kHz			-9999999	f10.3
60	X_Geofact	X_Geometric factor			-9999999	f10.3
61	EMZ_Raw[1]	Raw EMZ01 Window		(fT)	-9999999	f12.6
62	EMZ_Raw[2]	Raw EMZ02 Window		(fT)	-9999999	f12.6
63	EMZ_Raw[3]	Raw EMZ03 Window		(fT)	-9999999	f12.6
64	EMZ_Raw[4]	Raw EMZ04 Window		(fT)	-9999999	f12.6
65	EMZ_Raw[5]	Raw EMZ05 Window		(fT)	-9999999	f12.6
66	EMZ_Raw[6]	Raw EMZ06 Window		(fT)	-9999999	f12.6
67	EMZ_Raw[7]	Raw EMZ07 Window		(fT)	-9999999	f12.6
68	EMZ_Raw[8]	Raw EMZ08 Window		(fT)	-9999999	f12.6
69	EMZ_Raw[9]	Raw EMZ09 Window		(fT)	-9999999	f12.6
70	EMZ_Raw[10]	Raw EMZ10 Window		(fT)	-9999999	f12.6
71	EMZ_Raw[11]	Raw EMZ11 Window		(fT)	-9999999	f12.6
72	EMZ_Raw[12]	Raw EMZ12 Window		(fT)	-9999999	f12.6
73	EMZ_Raw[13]	Raw EMZ13 Window		(fT)	-9999999	f12.6
74	EMZ_Raw[14]	Raw EMZ14 Window		(fT)	-9999999	f12.6
75	EMZ_Raw[15]	Raw EMZ15 Window		(fT)	-9999999	f12.6
76	EMZ_Final[1]	Final EMZ01 Window		(fT)	-9999999	f12.6
77	EMZ_Final[2]	Final EMZ02 Window		(fT)	-9999999	f12.6
78	EMZ_Final[3]	Final EMZ03 Window		(fT)	-9999999	f12.6
79	EMZ_Final[4]	Final EMZ04 Window		(fT)	-9999999	f12.6
80	EMZ_Final[5]	Final EMZ05 Window		(fT)	-9999999	f12.6
81	EMZ_Final[6]	Final EMZ06 Window		(fT)	-9999999	f12.6
82	EMZ_Final[7]	Final EMZ07 Window		(fT)	-9999999	f12.6
83	EMZ_Final[8]	Final EMZ08 Window		(fT)	-9999999	f12.6
84	EMZ_Final[9]	Final EMZ09 Window		(fT)	-9999999	f12.6
85	EMZ_Final[10]	Final EMZ10 Window		(fT)	-9999999	f12.6
86	EMZ_Final[11]	Final EMZ11 Window		(fT)	-9999999	f12.6
87	EMZ_Final[12]	Final EMZ12 Window		(fT)	-9999999	f12.6
88	EMZ_Final[13]	Final EMZ13 Window		(fT)	-9999999	f12.6
89	EMZ_Final[14]	Final EMZ14 Window		(fT)	-9999999	f12.6
90	EMZ_Final[15]	Final EMZ15 Window		(fT)	-9999999	f12.6
91	Z_Sferics	Z_Sferics			-9999999	f10.3
92	Z_Lowfreq	Z_Lowfreq			-9999999	f10.3
93	Z_Powerline	Z_Powerline			-9999999	f10.3
94	Z_VLF1	Z_18.2kHz			-9999999	f10.3
95	Z_VLF2	Z_19.8kHz			-9999999	f10.3
96	Z_VLF3	Z_21.4kHz			-9999999	f10.3
97	Z_VLF4	Z_22.2kHz			-9999999	f10.3
98	Z_Geofact	Z_Geometric factor			-9999999	f10.3
99	CNDX[1]	Conductivity_X001	0-2	m	(mS/m)	-9999999 f10.3
100	CNDX[2]	Conductivity_X002	2-4	m	(mS/m)	-9999999 f10.3
101	CNDX[3]	Conductivity_X003	4-6	m	(mS/m)	-9999999 f10.3
102	CNDX[4]	Conductivity_X004	6-8	m	(mS/m)	-9999999 f10.3
103	CNDX[5]	Conductivity_X005	8-10	m	(mS/m)	-9999999 f10.3
104	CNDX[6]	Conductivity_X006	10-12	m	(mS/m)	-9999999 f10.3
105	CNDX[7]	Conductivity_X007	12-14	m	(mS/m)	-9999999 f10.3
106	CNDX[8]	Conductivity_X008	14-16	m	(mS/m)	-9999999 f10.3
107	CNDX[9]	Conductivity_X009	16-18	m	(mS/m)	-9999999 f10.3
108	CNDX[10]	Conductivity_X010	18-20	m	(mS/m)	-9999999 f10.3
109	CNDX[11]	Conductivity_X011	20-22	m	(mS/m)	-9999999 f10.3
110	CNDX[12]	Conductivity_X012	22-24	m	(mS/m)	-9999999 f10.3
111	CNDX[13]	Conductivity_X013	24-26	m	(mS/m)	-9999999 f10.3

112	CNDX[14]	Conductivity_X014	26-28	m	(mS/m)	-9999999	f10.3
113	CNDX[15]	Conductivity_X015	28-30	m	(mS/m)	-9999999	f10.3
114	CNDX[16]	Conductivity_X016	30-32	m	(mS/m)	-9999999	f10.3
115	CNDX[17]	Conductivity_X017	32-34	m	(mS/m)	-9999999	f10.3
116	CNDX[18]	Conductivity_X018	34-36	m	(mS/m)	-9999999	f10.3
117	CNDX[19]	Conductivity_X019	36-38	m	(mS/m)	-9999999	f10.3
118	CNDX[20]	Conductivity_X020	38-40	m	(mS/m)	-9999999	f10.3
119	CNDX[21]	Conductivity_X021	40-42	m	(mS/m)	-9999999	f10.3
120	CNDX[22]	Conductivity_X022	42-44	m	(mS/m)	-9999999	f10.3
121	CNDX[23]	Conductivity_X023	44-46	m	(mS/m)	-9999999	f10.3
122	CNDX[24]	Conductivity_X024	46-48	m	(mS/m)	-9999999	f10.3
123	CNDX[25]	Conductivity_X025	48-50	m	(mS/m)	-9999999	f10.3
124	CNDX[26]	Conductivity_X026	50-52	m	(mS/m)	-9999999	f10.3
125	CNDX[27]	Conductivity_X027	52-54	m	(mS/m)	-9999999	f10.3
126	CNDX[28]	Conductivity_X028	54-56	m	(mS/m)	-9999999	f10.3
127	CNDX[29]	Conductivity_X029	56-58	m	(mS/m)	-9999999	f10.3
128	CNDX[30]	Conductivity_X030	58-60	m	(mS/m)	-9999999	f10.3
129	CNDX[31]	Conductivity_X031	60-62	m	(mS/m)	-9999999	f10.3
130	CNDX[32]	Conductivity_X032	62-64	m	(mS/m)	-9999999	f10.3
131	CNDX[33]	Conductivity_X033	64-66	m	(mS/m)	-9999999	f10.3
132	CNDX[34]	Conductivity_X034	66-68	m	(mS/m)	-9999999	f10.3
133	CNDX[35]	Conductivity_X035	68-70	m	(mS/m)	-9999999	f10.3
134	CNDX[36]	Conductivity_X036	70-72	m	(mS/m)	-9999999	f10.3
135	CNDX[37]	Conductivity_X037	72-74	m	(mS/m)	-9999999	f10.3
136	CNDX[38]	Conductivity_X038	74-76	m	(mS/m)	-9999999	f10.3
137	CNDX[39]	Conductivity_X039	76-78	m	(mS/m)	-9999999	f10.3
138	CNDX[40]	Conductivity_X040	78-80	m	(mS/m)	-9999999	f10.3
139	CNDX[41]	Conductivity_X041	80-82	m	(mS/m)	-9999999	f10.3
140	CNDX[42]	Conductivity_X042	82-84	m	(mS/m)	-9999999	f10.3
141	CNDX[43]	Conductivity_X043	84-86	m	(mS/m)	-9999999	f10.3
142	CNDX[44]	Conductivity_X044	86-88	m	(mS/m)	-9999999	f10.3
143	CNDX[45]	Conductivity_X045	88-90	m	(mS/m)	-9999999	f10.3
144	CNDX[46]	Conductivity_X046	90-92	m	(mS/m)	-9999999	f10.3
145	CNDX[47]	Conductivity_X047	92-94	m	(mS/m)	-9999999	f10.3
146	CNDX[48]	Conductivity_X048	94-96	m	(mS/m)	-9999999	f10.3
147	CNDX[49]	Conductivity_X049	96-98	m	(mS/m)	-9999999	f10.3
148	CNDX[50]	Conductivity_X050	98-100	m	(mS/m)	-9999999	f10.3
149	CNDX[51]	Conductivity_X051	100-102	m	(mS/m)	-9999999	f10.3
150	CNDX[52]	Conductivity_X052	102-104	m	(mS/m)	-9999999	f10.3
151	CNDX[53]	Conductivity_X053	104-106	m	(mS/m)	-9999999	f10.3
152	CNDX[54]	Conductivity_X054	106-108	m	(mS/m)	-9999999	f10.3
153	CNDX[55]	Conductivity_X055	108-110	m	(mS/m)	-9999999	f10.3
154	CNDX[56]	Conductivity_X056	110-112	m	(mS/m)	-9999999	f10.3
155	CNDX[57]	Conductivity_X057	112-114	m	(mS/m)	-9999999	f10.3
156	CNDX[58]	Conductivity_X058	114-116	m	(mS/m)	-9999999	f10.3
157	CNDX[59]	Conductivity_X059	116-118	m	(mS/m)	-9999999	f10.3
158	CNDX[60]	Conductivity_X060	118-120	m	(mS/m)	-9999999	f10.3
159	CNDX[61]	Conductivity_X061	120-122	m	(mS/m)	-9999999	f10.3
160	CNDX[62]	Conductivity_X062	122-124	m	(mS/m)	-9999999	f10.3
161	CNDX[63]	Conductivity_X063	124-126	m	(mS/m)	-9999999	f10.3
162	CNDX[64]	Conductivity_X064	126-128	m	(mS/m)	-9999999	f10.3
163	CNDX[65]	Conductivity_X065	128-130	m	(mS/m)	-9999999	f10.3
164	CNDX[66]	Conductivity_X066	130-132	m	(mS/m)	-9999999	f10.3
165	CNDX[67]	Conductivity_X067	132-134	m	(mS/m)	-9999999	f10.3
166	CNDX[68]	Conductivity_X068	134-136	m	(mS/m)	-9999999	f10.3
167	CNDX[69]	Conductivity_X069	136-138	m	(mS/m)	-9999999	f10.3
168	CNDX[70]	Conductivity_X070	138-140	m	(mS/m)	-9999999	f10.3
169	CNDX[71]	Conductivity_X071	140-142	m	(mS/m)	-9999999	f10.3
170	CNDX[72]	Conductivity_X072	142-144	m	(mS/m)	-9999999	f10.3
171	CNDX[73]	Conductivity_X073	144-146	m	(mS/m)	-9999999	f10.3
172	CNDX[74]	Conductivity_X074	146-148	m	(mS/m)	-9999999	f10.3
173	CNDX[75]	Conductivity_X075	148-150	m	(mS/m)	-9999999	f10.3
174	CNDX[76]	Conductivity_X076	150-152	m	(mS/m)	-9999999	f10.3
175	CNDX[77]	Conductivity_X077	152-154	m	(mS/m)	-9999999	f10.3

176	CNDX[78]	Conductivity_X078	154-156 m	(mS/m)	-9999999	f10.3
177	CNDX[79]	Conductivity_X079	156-158 m	(mS/m)	-9999999	f10.3
178	CNDX[80]	Conductivity_X080	158-160 m	(mS/m)	-9999999	f10.3
179	CNDX[81]	Conductivity_X081	160-162 m	(mS/m)	-9999999	f10.3
180	CNDX[82]	Conductivity_X082	162-164 m	(mS/m)	-9999999	f10.3
181	CNDX[83]	Conductivity_X083	164-166 m	(mS/m)	-9999999	f10.3
182	CNDX[84]	Conductivity_X084	166-168 m	(mS/m)	-9999999	f10.3
183	CNDX[85]	Conductivity_X085	168-170 m	(mS/m)	-9999999	f10.3
184	CNDX[86]	Conductivity_X086	170-172 m	(mS/m)	-9999999	f10.3
185	CNDX[87]	Conductivity_X087	172-174 m	(mS/m)	-9999999	f10.3
186	CNDX[88]	Conductivity_X088	174-176 m	(mS/m)	-9999999	f10.3
187	CNDX[89]	Conductivity_X089	176-178 m	(mS/m)	-9999999	f10.3
188	CNDX[90]	Conductivity_X090	178-180 m	(mS/m)	-9999999	f10.3
189	CNDX[91]	Conductivity_X091	180-182 m	(mS/m)	-9999999	f10.3
190	CNDX[92]	Conductivity_X092	182-184 m	(mS/m)	-9999999	f10.3
191	CNDX[93]	Conductivity_X093	184-186 m	(mS/m)	-9999999	f10.3
192	CNDX[94]	Conductivity_X094	186-188 m	(mS/m)	-9999999	f10.3
193	CNDX[95]	Conductivity_X095	188-190 m	(mS/m)	-9999999	f10.3
194	CNDX[96]	Conductivity_X096	190-192 m	(mS/m)	-9999999	f10.3
195	CNDX[97]	Conductivity_X097	192-194 m	(mS/m)	-9999999	f10.3
196	CNDX[98]	Conductivity_X098	194-196 m	(mS/m)	-9999999	f10.3
197	CNDX[99]	Conductivity_X099	196-198 m	(mS/m)	-9999999	f10.3
198	CNDX[100]	Conductivity_X100	198-200 m	(mS/m)	-9999999	f10.3

COMM

COMM Total number of lines : 9

COMM

COMM	Flt	Line	Start X	Start Y	End X	End Y	Kms
------	-----	------	---------	---------	-------	-------	-----

COMM

COMM	2	10023	274941	7463991	274960	7473201	9.21
COMM	2	10031	264996	7473102	264996	7460214	12.89
COMM	2	10040	255033	7454466	255029	7471058	16.59
COMM	2	10052	245004	7469083	245009	7454364	14.72
COMM	1	10060	234979	7452286	234969	7468868	16.58
COMM	1	10070	225015	7468722	225018	7452084	16.64
COMM	1	10080	215001	7451878	214996	7468486	16.61
COMM	1	10090	204976	7468385	204965	7451753	16.63
COMM	1	10100	194999	7451508	195001	7463136	11.63

COMM

COMM Total Kilometres : 131.50

**SCIMITAR RESOURCES LIMITED**

COMM JOB NUMBER: 1900

COMM AREA NUMBER: 1

COMM SURVEY COMPANY: Fugro Airborne Surveys

COMM CLIENT: Scimitar Resources Limited

COMM SURVEY TYPE: 25Hz TEMPEST Survey

COMM AREA NAME: Southern NT

COMM STATE: NT

COMM COUNTRY: Australia

COMM SURVEY FLOWN: July, 2007

COMM LOCATED DATA CREATED: Aug 2007

COMM

COMM DATUM: GDA94

COMM PROJECTION: MGA

COMM ZONE: 53

COMM

COMM SURVEY SPECIFICATIONS

COMM

COMM TRAVERSE LINE SPACING: variable

COMM TRAVERSE LINE DIRECTION: variable

COMM TIE LINE SPACING: n/a

COMM TIE LINE DIRECTION: n/a

COMM NOMINAL TERRAIN CLEARANCE: 120 m  
 COMM FINAL LINE KILOMETRES: 413 km  
 COMM  
 COMM LINE NUMBERING  
 COMM  
 COMM TRAVERSE LINE NUMBERS: 10010 - 10121  
 COMM TIE LINE NUMBERS: n/a  
 COMM  
 COMM SURVEY EQUIPMENT  
 COMM  
 COMM AIRCRAFT: CASA C212 Turbo Prop, TEM  
 COMM  
 COMM MAGNETOMETER: Scintrex Cs-2 Cesium Vapour  
 COMM INSTALLATION: stinger mount  
 COMM RESOLUTION: 0.001 nT  
 COMM RECORDING INTERVAL: 0.2 s  
 COMM  
 COMM ELECTROMAGNETIC SYSTEM: 25Hz TEMPEST  
 COMM INSTALLATION: Transmitter loop mounted on the aircraft  
 COMM Receiver coils in a towed bird  
 COMM COIL ORIENTATION: X,Z  
 COMM RECORDING INTERVAL: 0.2 s  
 COMM SYSTEM GEOMETRY:  
 COMM RECEIVER DISTANCE BEHIND THE TRANSMITTER: -120 m  
 COMM RECEIVER DISTANCE BELOW THE TRANSMITTER: -35 m  
 COMM  
 COMM RADAR ALTIMETER: Sperry RT-220  
 COMM RECORDING INTERVAL: 0.2 s  
 COMM  
 COMM NAVIGATION: real-time differential GPS  
 COMM RECORDING INTERVAL: 1.0 s  
 COMM  
 COMM ACQUISITION SYSTEM: PDAS-1000  
 COMM  
 COMM DATA PROCESSING  
 COMM  
 COMM MAGNETIC DATA  
 COMM DIURNAL BASE VALUE APPLIED 53325 nT  
 COMM PARALLAX CORRECTION APPLIED 0.6 s  
 COMM IGRF BASE VALUE APPLIED 52942 nT  
 COMM IGRF MODEL 2005 EXTRAPOLATED TO 2007.5  
 COMM  
 COMM ELECTROMAGNETIC DATA  
 COMM SYSTEM PARALLAX REMOVED, AS FOLLOWS  
 COMM X-COMPONENT EM DATA 0.2 s  
 COMM Z-COMPONENT EM DATA 1.4 s  
 COMM DATA CORRECTED FOR TRANSMITTER HEIGHT, PITCH AND ROLL  
 COMM DATA CORRECTED FOR TRANSMITTER-RECEIVER GEOMETRY VARIATIONS  
 COMM CONDUCTIVITY DEPTH INVERSION CALCULATED EMFlow V5.10  
 COMM CONDUCTIVITIES CALCULATED USING corrected EM DATA  
 COMM  
 COMM DIGITAL TERRAIN DATA  
 COMM PARALLAX CORRECTION APPLIED TO RADAR ALIMETER DATA 0.6 s  
 COMM PARALLAX CORRECTION APPLIED TO GPS ALIMETER DATA 0.0 s  
 COMM DTM CALCULATED [DTM = GPS ALTITUDE - RADAR ALTITUDE]  
 COMM -----  
 COMM The accuracy of the elevation calculation is directly dependent on  
 COMM the accuracy of the two input parameters, radar altitude and GPS  
 COMM altitude. The radar altitude value may be erroneous in areas of heavy  
 COMM tree cover, where the altimeter reflects the distance to the tree  
 COMM canopy rather than the ground. The GPS altitude value is primarily  
 COMM dependent on the number of available satellites. Although  
 COMM post-processing of GPS data will yield X and Y accuracies in the  
 COMM order of 1-2 metres, the accuracy of the altitude value is usually

COMM much less, sometimes in the  $\pm 5$  metre range. Further inaccuracies  
 COMM may be introduced during the interpolation and gridding process.  
 COMM Because of the inherent inaccuracies of this method, no guarantee is  
 COMM made or implied that the information displayed is a true  
 COMM representation of the height above sea level. Although this product  
 COMM may be of some use as a general reference,  
 COMM THIS PRODUCT MUST NOT BE USED FOR NAVIGATION PURPOSES.

COMM -----

COMM

COMM ELECTROMAGNETIC SYSTEM

COMM

COMM TEMPEST IS A TIME-DOMAIN SQUARE-WAVE SYSTEM,  
 COMM TRANSMITTING AT A BASE FREQUENCY OF 25Hz,  
 COMM WITH 2 ORTHOGONAL-AXIS RECEIVER COILS IN A TOWED BIRD.  
 COMM FINAL EM OUTPUT IS RECORDED 5 TIMES PER SECOND.  
 COMM THE TIMES (IN MILLISECONDS) FOR THE 15 WINDOWS ARE:

COMM

COMM WINDOW	START	END	CENTRE
COMM 1	0.007	0.020	0.013
COMM 2	0.033	0.047	0.040
COMM 3	0.060	0.073	0.067
COMM 4	0.087	0.127	0.107
COMM 5	0.140	0.207	0.173
COMM 6	0.220	0.340	0.280
COMM 7	0.353	0.553	0.453
COMM 8	0.567	0.873	0.720
COMM 9	0.887	1.353	1.120
COMM 10	1.367	2.100	1.733
COMM 11	2.113	3.273	2.693
COMM 12	3.287	5.113	4.200
COMM 13	5.127	7.993	6.560
COMM 14	8.007	12.393	10.200
COMM 15	12.407	19.993	16.200

COMM

COMM PULSE WIDTH: 10 ms

COMM

COMM TEMPEST EM data are transformed to the response that would be  
 COMM obtained with a B-field sensor for a 100% duty cycle square  
 COMM waveform at the base frequency, involving a 1A change in  
 COMM current (from -0.5A to +0.5A to -0.5A) in a 1sq.m transmitter.  
 COMM It is this configuration, rather than the actual acquisition  
 COMM configuration, which must be specified when modelling TEMPEST data.

COMM

COMM

#### LOCATED DATA FORMAT

Output field format : DOS - Flat ascii  
 Number of fields : 198

Field	Channel	Description	Units	Undefined
Format				
----	-----	-----	-----	-----
1	LINE	Line		-9999999 i6
2	FLIGHT	Flight		-9999999 i4
3	FID	Fiducial	(s)	-9999999 f8.1
4	LATITUDE	Latitude GDA94	(deg)	-9999999 f13.6
5	LONGITUDE	Longitude GDA94	(deg)	-9999999 f13.6
6	EASTING	Easting MGA53	(m)	-9999999 f11.2
7	NORTHING	Northing MGA53	(m)	-9999999 f12.2
8	TxHeight	GPS height	(m)	-9999999 f8.2
9	Baro	Barometric Altitude	(m)	-9999999 f8.2
10	TxRalt_raw	Raw Radar Altimeter	(m)	-9999999 f8.2

11	TxRalt_final	Final Radar Altimeter	(m)	-9999999	f8.2
12	DTM	DTM	(m)	-9999999	f8.2
13	MAG	Compensated TMI	(nT)	-9999999	f10.3
14	MAG_1VD	Levelled TMI 1VD	(nT/m)	-9999999	f12.5
15	Pitch_Raw	Raw Tx loop pitch	(deg)	-9999999	f10.5
16	Roll_Raw	Raw Tx loop roll	(deg)	-9999999	f10.5
17	HSep_Raw	Raw Tx-Rx horizontal separation	(m)	-9999999	f8.2
18	VSep_Raw	Raw Tx-Rx vertical separation	(m)	-9999999	f8.2
19	Pitch_Final	Final Tx loop pitch	(deg)	-9999999	f10.5
20	Roll_Final	Final Tx loop roll	(deg)	-9999999	f10.5
21	HSep_Final	Final Tx-Rx horizontal separation	(m)	-9999999	f8.2
22	VSep_Final	Final Tx-Rx vertical separation	(m)	-9999999	f8.2
23	EMX_Raw[1]	Raw EMX01 Window	(fT)	-9999999	f12.6
24	EMX_Raw[2]	Raw EMX02 Window	(fT)	-9999999	f12.6
25	EMX_Raw[3]	Raw EMX03 Window	(fT)	-9999999	f12.6
26	EMX_Raw[4]	Raw EMX04 Window	(fT)	-9999999	f12.6
27	EMX_Raw[5]	Raw EMX05 Window	(fT)	-9999999	f12.6
28	EMX_Raw[6]	Raw EMX06 Window	(fT)	-9999999	f12.6
29	EMX_Raw[7]	Raw EMX07 Window	(fT)	-9999999	f12.6
30	EMX_Raw[8]	Raw EMX08 Window	(fT)	-9999999	f12.6
31	EMX_Raw[9]	Raw EMX09 Window	(fT)	-9999999	f12.6
32	EMX_Raw[10]	Raw EMX10 Window	(fT)	-9999999	f12.6
33	EMX_Raw[11]	Raw EMX11 Window	(fT)	-9999999	f12.6
34	EMX_Raw[12]	Raw EMX12 Window	(fT)	-9999999	f12.6
35	EMX_Raw[13]	Raw EMX13 Window	(fT)	-9999999	f12.6
36	EMX_Raw[14]	Raw EMX14 Window	(fT)	-9999999	f12.6
37	EMX_Raw[15]	Raw EMX15 Window	(fT)	-9999999	f12.6
38	EMX_Final[1]	Final EMX01 Window	(fT)	-9999999	f12.6
39	EMX_Final[2]	Final EMX02 Window	(fT)	-9999999	f12.6
40	EMX_Final[3]	Final EMX03 Window	(fT)	-9999999	f12.6
41	EMX_Final[4]	Final EMX04 Window	(fT)	-9999999	f12.6
42	EMX_Final[5]	Final EMX05 Window	(fT)	-9999999	f12.6
43	EMX_Final[6]	Final EMX06 Window	(fT)	-9999999	f12.6
44	EMX_Final[7]	Final EMX07 Window	(fT)	-9999999	f12.6
45	EMX_Final[8]	Final EMX08 Window	(fT)	-9999999	f12.6
46	EMX_Final[9]	Final EMX09 Window	(fT)	-9999999	f12.6
47	EMX_Final[10]	Final EMX10 Window	(fT)	-9999999	f12.6
48	EMX_Final[11]	Final EMX11 Window	(fT)	-9999999	f12.6
49	EMX_Final[12]	Final EMX12 Window	(fT)	-9999999	f12.6
50	EMX_Final[13]	Final EMX13 Window	(fT)	-9999999	f12.6
51	EMX_Final[14]	Final EMX14 Window	(fT)	-9999999	f12.6
52	EMX_Final[15]	Final EMX15 Window	(fT)	-9999999	f12.6
53	X_Sferics	X_Sferics		-9999999	f10.3
54	X_Lowfreq	X_Lowfreq		-9999999	f10.3
55	X_Powerline	X_Powerline		-9999999	f10.3
56	X_VLF1	X_18.2kHz		-9999999	f10.3
57	X_VLF2	X_19.8kHz		-9999999	f10.3
58	X_VLF3	X_21.4kHz		-9999999	f10.3
59	X_VLF4	X_22.2kHz		-9999999	f10.3
60	X_Geofact	X_Geometric factor		-9999999	f10.3
61	EMZ_Raw[1]	Raw EMZ01 Window	(fT)	-9999999	f12.6
62	EMZ_Raw[2]	Raw EMZ02 Window	(fT)	-9999999	f12.6
63	EMZ_Raw[3]	Raw EMZ03 Window	(fT)	-9999999	f12.6
64	EMZ_Raw[4]	Raw EMZ04 Window	(fT)	-9999999	f12.6
65	EMZ_Raw[5]	Raw EMZ05 Window	(fT)	-9999999	f12.6
66	EMZ_Raw[6]	Raw EMZ06 Window	(fT)	-9999999	f12.6
67	EMZ_Raw[7]	Raw EMZ07 Window	(fT)	-9999999	f12.6
68	EMZ_Raw[8]	Raw EMZ08 Window	(fT)	-9999999	f12.6
69	EMZ_Raw[9]	Raw EMZ09 Window	(fT)	-9999999	f12.6
70	EMZ_Raw[10]	Raw EMZ10 Window	(fT)	-9999999	f12.6
71	EMZ_Raw[11]	Raw EMZ11 Window	(fT)	-9999999	f12.6
72	EMZ_Raw[12]	Raw EMZ12 Window	(fT)	-9999999	f12.6
73	EMZ_Raw[13]	Raw EMZ13 Window	(fT)	-9999999	f12.6
74	EMZ_Raw[14]	Raw EMZ14 Window	(fT)	-9999999	f12.6

75	EMZ_Raw[15]	Raw EMZ15 Window	(fT)	-9999999	f12.6
76	EMZ_Final[1]	Final EMZ01 Window	(fT)	-9999999	f12.6
77	EMZ_Final[2]	Final EMZ02 Window	(fT)	-9999999	f12.6
78	EMZ_Final[3]	Final EMZ03 Window	(fT)	-9999999	f12.6
79	EMZ_Final[4]	Final EMZ04 Window	(fT)	-9999999	f12.6
80	EMZ_Final[5]	Final EMZ05 Window	(fT)	-9999999	f12.6
81	EMZ_Final[6]	Final EMZ06 Window	(fT)	-9999999	f12.6
82	EMZ_Final[7]	Final EMZ07 Window	(fT)	-9999999	f12.6
83	EMZ_Final[8]	Final EMZ08 Window	(fT)	-9999999	f12.6
84	EMZ_Final[9]	Final EMZ09 Window	(fT)	-9999999	f12.6
85	EMZ_Final[10]	Final EMZ10 Window	(fT)	-9999999	f12.6
86	EMZ_Final[11]	Final EMZ11 Window	(fT)	-9999999	f12.6
87	EMZ_Final[12]	Final EMZ12 Window	(fT)	-9999999	f12.6
88	EMZ_Final[13]	Final EMZ13 Window	(fT)	-9999999	f12.6
89	EMZ_Final[14]	Final EMZ14 Window	(fT)	-9999999	f12.6
90	EMZ_Final[15]	Final EMZ15 Window	(fT)	-9999999	f12.6
91	Z_Sferics	Z_Sferics		-9999999	f10.3
92	Z_Lowfreq	Z_Lowfreq		-9999999	f10.3
93	Z_Powerline	Z_Powerline		-9999999	f10.3
94	Z_VLF1	Z_18.2kHz		-9999999	f10.3
95	Z_VLF2	Z_19.8kHz		-9999999	f10.3
96	Z_VLF3	Z_21.4kHz		-9999999	f10.3
97	Z_VLF4	Z_22.2kHz		-9999999	f10.3
98	Z_Geofact	Z_Geometric factor		-9999999	f10.3
99	CNDX[1]	Conductivity_X001	0-2 m (mS/m)	-9999999	f10.3
100	CNDX[2]	Conductivity_X002	2-4 m (mS/m)	-9999999	f10.3
101	CNDX[3]	Conductivity_X003	4-6 m (mS/m)	-9999999	f10.3
102	CNDX[4]	Conductivity_X004	6-8 m (mS/m)	-9999999	f10.3
103	CNDX[5]	Conductivity_X005	8-10 m (mS/m)	-9999999	f10.3
104	CNDX[6]	Conductivity_X006	10-12 m (mS/m)	-9999999	f10.3
105	CNDX[7]	Conductivity_X007	12-14 m (mS/m)	-9999999	f10.3
106	CNDX[8]	Conductivity_X008	14-16 m (mS/m)	-9999999	f10.3
107	CNDX[9]	Conductivity_X009	16-18 m (mS/m)	-9999999	f10.3
108	CNDX[10]	Conductivity_X010	18-20 m (mS/m)	-9999999	f10.3
109	CNDX[11]	Conductivity_X011	20-22 m (mS/m)	-9999999	f10.3
110	CNDX[12]	Conductivity_X012	22-24 m (mS/m)	-9999999	f10.3
111	CNDX[13]	Conductivity_X013	24-26 m (mS/m)	-9999999	f10.3
112	CNDX[14]	Conductivity_X014	26-28 m (mS/m)	-9999999	f10.3
113	CNDX[15]	Conductivity_X015	28-30 m (mS/m)	-9999999	f10.3
114	CNDX[16]	Conductivity_X016	30-32 m (mS/m)	-9999999	f10.3
115	CNDX[17]	Conductivity_X017	32-34 m (mS/m)	-9999999	f10.3
116	CNDX[18]	Conductivity_X018	34-36 m (mS/m)	-9999999	f10.3
117	CNDX[19]	Conductivity_X019	36-38 m (mS/m)	-9999999	f10.3
118	CNDX[20]	Conductivity_X020	38-40 m (mS/m)	-9999999	f10.3
119	CNDX[21]	Conductivity_X021	40-42 m (mS/m)	-9999999	f10.3
120	CNDX[22]	Conductivity_X022	42-44 m (mS/m)	-9999999	f10.3
121	CNDX[23]	Conductivity_X023	44-46 m (mS/m)	-9999999	f10.3
122	CNDX[24]	Conductivity_X024	46-48 m (mS/m)	-9999999	f10.3
123	CNDX[25]	Conductivity_X025	48-50 m (mS/m)	-9999999	f10.3
124	CNDX[26]	Conductivity_X026	50-52 m (mS/m)	-9999999	f10.3
125	CNDX[27]	Conductivity_X027	52-54 m (mS/m)	-9999999	f10.3
126	CNDX[28]	Conductivity_X028	54-56 m (mS/m)	-9999999	f10.3
127	CNDX[29]	Conductivity_X029	56-58 m (mS/m)	-9999999	f10.3
128	CNDX[30]	Conductivity_X030	58-60 m (mS/m)	-9999999	f10.3
129	CNDX[31]	Conductivity_X031	60-62 m (mS/m)	-9999999	f10.3
130	CNDX[32]	Conductivity_X032	62-64 m (mS/m)	-9999999	f10.3
131	CNDX[33]	Conductivity_X033	64-66 m (mS/m)	-9999999	f10.3
132	CNDX[34]	Conductivity_X034	66-68 m (mS/m)	-9999999	f10.3
133	CNDX[35]	Conductivity_X035	68-70 m (mS/m)	-9999999	f10.3
134	CNDX[36]	Conductivity_X036	70-72 m (mS/m)	-9999999	f10.3
135	CNDX[37]	Conductivity_X037	72-74 m (mS/m)	-9999999	f10.3
136	CNDX[38]	Conductivity_X038	74-76 m (mS/m)	-9999999	f10.3
137	CNDX[39]	Conductivity_X039	76-78 m (mS/m)	-9999999	f10.3
138	CNDX[40]	Conductivity_X040	78-80 m (mS/m)	-9999999	f10.3

139	CNDX[41]	Conductivity_X041	80-82	m	(mS/m)	-9999999	f10.3
140	CNDX[42]	Conductivity_X042	82-84	m	(mS/m)	-9999999	f10.3
141	CNDX[43]	Conductivity_X043	84-86	m	(mS/m)	-9999999	f10.3
142	CNDX[44]	Conductivity_X044	86-88	m	(mS/m)	-9999999	f10.3
143	CNDX[45]	Conductivity_X045	88-90	m	(mS/m)	-9999999	f10.3
144	CNDX[46]	Conductivity_X046	90-92	m	(mS/m)	-9999999	f10.3
145	CNDX[47]	Conductivity_X047	92-94	m	(mS/m)	-9999999	f10.3
146	CNDX[48]	Conductivity_X048	94-96	m	(mS/m)	-9999999	f10.3
147	CNDX[49]	Conductivity_X049	96-98	m	(mS/m)	-9999999	f10.3
148	CNDX[50]	Conductivity_X050	98-100	m	(mS/m)	-9999999	f10.3
149	CNDX[51]	Conductivity_X051	100-102	m	(mS/m)	-9999999	f10.3
150	CNDX[52]	Conductivity_X052	102-104	m	(mS/m)	-9999999	f10.3
151	CNDX[53]	Conductivity_X053	104-106	m	(mS/m)	-9999999	f10.3
152	CNDX[54]	Conductivity_X054	106-108	m	(mS/m)	-9999999	f10.3
153	CNDX[55]	Conductivity_X055	108-110	m	(mS/m)	-9999999	f10.3
154	CNDX[56]	Conductivity_X056	110-112	m	(mS/m)	-9999999	f10.3
155	CNDX[57]	Conductivity_X057	112-114	m	(mS/m)	-9999999	f10.3
156	CNDX[58]	Conductivity_X058	114-116	m	(mS/m)	-9999999	f10.3
157	CNDX[59]	Conductivity_X059	116-118	m	(mS/m)	-9999999	f10.3
158	CNDX[60]	Conductivity_X060	118-120	m	(mS/m)	-9999999	f10.3
159	CNDX[61]	Conductivity_X061	120-122	m	(mS/m)	-9999999	f10.3
160	CNDX[62]	Conductivity_X062	122-124	m	(mS/m)	-9999999	f10.3
161	CNDX[63]	Conductivity_X063	124-126	m	(mS/m)	-9999999	f10.3
162	CNDX[64]	Conductivity_X064	126-128	m	(mS/m)	-9999999	f10.3
163	CNDX[65]	Conductivity_X065	128-130	m	(mS/m)	-9999999	f10.3
164	CNDX[66]	Conductivity_X066	130-132	m	(mS/m)	-9999999	f10.3
165	CNDX[67]	Conductivity_X067	132-134	m	(mS/m)	-9999999	f10.3
166	CNDX[68]	Conductivity_X068	134-136	m	(mS/m)	-9999999	f10.3
167	CNDX[69]	Conductivity_X069	136-138	m	(mS/m)	-9999999	f10.3
168	CNDX[70]	Conductivity_X070	138-140	m	(mS/m)	-9999999	f10.3
169	CNDX[71]	Conductivity_X071	140-142	m	(mS/m)	-9999999	f10.3
170	CNDX[72]	Conductivity_X072	142-144	m	(mS/m)	-9999999	f10.3
171	CNDX[73]	Conductivity_X073	144-146	m	(mS/m)	-9999999	f10.3
172	CNDX[74]	Conductivity_X074	146-148	m	(mS/m)	-9999999	f10.3
173	CNDX[75]	Conductivity_X075	148-150	m	(mS/m)	-9999999	f10.3
174	CNDX[76]	Conductivity_X076	150-152	m	(mS/m)	-9999999	f10.3
175	CNDX[77]	Conductivity_X077	152-154	m	(mS/m)	-9999999	f10.3
176	CNDX[78]	Conductivity_X078	154-156	m	(mS/m)	-9999999	f10.3
177	CNDX[79]	Conductivity_X079	156-158	m	(mS/m)	-9999999	f10.3
178	CNDX[80]	Conductivity_X080	158-160	m	(mS/m)	-9999999	f10.3
179	CNDX[81]	Conductivity_X081	160-162	m	(mS/m)	-9999999	f10.3
180	CNDX[82]	Conductivity_X082	162-164	m	(mS/m)	-9999999	f10.3
181	CNDX[83]	Conductivity_X083	164-166	m	(mS/m)	-9999999	f10.3
182	CNDX[84]	Conductivity_X084	166-168	m	(mS/m)	-9999999	f10.3
183	CNDX[85]	Conductivity_X085	168-170	m	(mS/m)	-9999999	f10.3
184	CNDX[86]	Conductivity_X086	170-172	m	(mS/m)	-9999999	f10.3
185	CNDX[87]	Conductivity_X087	172-174	m	(mS/m)	-9999999	f10.3
186	CNDX[88]	Conductivity_X088	174-176	m	(mS/m)	-9999999	f10.3
187	CNDX[89]	Conductivity_X089	176-178	m	(mS/m)	-9999999	f10.3
188	CNDX[90]	Conductivity_X090	178-180	m	(mS/m)	-9999999	f10.3
189	CNDX[91]	Conductivity_X091	180-182	m	(mS/m)	-9999999	f10.3
190	CNDX[92]	Conductivity_X092	182-184	m	(mS/m)	-9999999	f10.3
191	CNDX[93]	Conductivity_X093	184-186	m	(mS/m)	-9999999	f10.3
192	CNDX[94]	Conductivity_X094	186-188	m	(mS/m)	-9999999	f10.3
193	CNDX[95]	Conductivity_X095	188-190	m	(mS/m)	-9999999	f10.3
194	CNDX[96]	Conductivity_X096	190-192	m	(mS/m)	-9999999	f10.3
195	CNDX[97]	Conductivity_X097	192-194	m	(mS/m)	-9999999	f10.3
196	CNDX[98]	Conductivity_X098	194-196	m	(mS/m)	-9999999	f10.3
197	CNDX[99]	Conductivity_X099	196-198	m	(mS/m)	-9999999	f10.3
198	CNDX[100]	Conductivity_X100	198-200	m	(mS/m)	-9999999	f10.3

COMM

COMM Total number of lines : 15

COMM

COMM Flt Line Start X Start Y End X End Y Kms

COMM							
COMM	1	10120	299823	7444851	181703	7444874	118.12
COMM	1	10100	194992	7439986	194998	7451440	11.45
COMM	1	10070	225018	7452150	225018	7440037	12.11
COMM	1	10060	234975	7439984	234980	7452216	12.23
COMM	1	10061	234969	7468868	234992	7481796	12.93
COMM	2	10031	264993	7491733	264996	7473168	18.57
COMM	2	10032	264996	7460214	264995	7440027	20.19
COMM	2	10040	255037	7440044	255034	7454536	14.49
COMM	2	10041	255029	7471058	255039	7476635	5.58
COMM	2	10110	227256	7474969	299465	7475161	72.21
COMM	2	10052	244872	7476509	245003	7469150	7.36
COMM	2	10053	245009	7454430	245005	7440029	14.40
COMM	2	10024	274958	7439845	274941	7463991	24.15
COMM	2	10023	274960	7473201	274949	7491622	18.42
COMM	2	10010	290085	7491816	290090	7440455	51.36
COMM							
COMM	Total Kilometres :			413.57			

**COMBINED DATA**

COMM JOB NUMBER:	1900
COMM AREA NUMBER:	1
COMM SURVEY COMPANY:	Fugro Airborne Surveys
COMM CLIENT:	Scimitar Resources Limited / Toro Energy Limited
COMM SURVEY TYPE:	25Hz TEMPEST Survey
COMM AREA NAME:	Southern NT
COMM STATE:	NT
COMM COUNTRY:	Australia
COMM SURVEY FLOWN:	July, 2007
COMM LOCATED DATA CREATED:	Aug 2007
COMM	
COMM DATUM:	GDA94
COMM PROJECTION:	MGA
COMM ZONE:	53
COMM	
COMM SURVEY SPECIFICATIONS	
COMM	
COMM TRAVERSE LINE SPACING:	variable
COMM TRAVERSE LINE DIRECTION:	variable
COMM TIE LINE SPACING:	n/a
COMM TIE LINE DIRECTION:	n/a
COMM NOMINAL TERRAIN CLEARANCE:	120 m
COMM FINAL LINE KILOMETRES:	550 km
COMM	
COMM LINE NUMBERING	
COMM	
COMM TRAVERSE LINE NUMBERS:	10010 - 10121
COMM TIE LINE NUMBERS:	n/a
COMM	
COMM SURVEY EQUIPMENT	
COMM	
COMM AIRCRAFT:	CASA C212 Turbo Prop, TEM
COMM	
COMM MAGNETOMETER:	Scintrex Cs-2 Cesium Vapour
COMM INSTALLATION:	stinger mount
COMM RESOLUTION:	0.001 nT
COMM RECORDING INTERVAL:	0.2 s
COMM	
COMM ELECTROMAGNETIC SYSTEM:	25Hz TEMPEST
COMM INSTALLATION:	Transmitter loop mounted on the aircraft
COMM	Receiver coils in a towed bird
COMM COIL ORIENTATION:	X,Z

```

COMM RECORDING INTERVAL:                                0.2 s
COMM SYSTEM GEOMETRY:
COMM RECEIVER DISTANCE BEHIND THE TRANSMITTER:          -120 m
COMM RECEIVER DISTANCE BELOW THE TRANSMITTER:           -35 m
COMM
COMM RADAR ALTIMETER:                                    Sperry RT-220
COMM RECORDING INTERVAL:                                0.2 s
COMM
COMM NAVIGATION:                                         real-time differential GPS
COMM RECORDING INTERVAL:                                1.0 s
COMM
COMM ACQUISITION SYSTEM:                                PDAS-1000
COMM
COMM DATA PROCESSING
COMM
COMM MAGNETIC DATA
COMM DIURNAL BASE VALUE APPLIED                          53325 nT
COMM PARALLAX CORRECTION APPLIED                          0.6 s
COMM IGRF BASE VALUE APPLIED                             52942 nT
COMM IGRF MODEL 2005 EXTRAPOLATED TO                     2007.5
COMM
COMM ELECTROMAGNETIC DATA
COMM SYSTEM PARALLAX REMOVED, AS FOLLOWS
COMM X-COMPONENT EM DATA                                0.2 s
COMM Z-COMPONENT EM DATA                                1.4 s
COMM DATA CORRECTED FOR TRANSMITTER HEIGHT, PITCH AND ROLL
COMM DATA CORRECTED FOR TRANSMITTER-RECEIVER GEOMETRY VARIATIONS
COMM CONDUCTIVITY DEPTH INVERSION CALCULATED             EMFlow V5.10
COMM CONDUCTIVITIES CALCULATED USING corrected EM DATA
COMM
COMM DIGITAL TERRAIN DATA
COMM PARALLAX CORRECTION APPLIED TO RADAR ALIMETER DATA 0.6 s
COMM PARALLAX CORRECTION APPLIED TO GPS ALIMETER DATA   0.0 s
COMM DTM CALCULATED [DTM = GPS ALTITUDE - RADAR ALTITUDE]
COMM -----
COMM The accuracy of the elevation calculation is directly dependent on
COMM the accuracy of the two input parameters, radar altitude and GPS
COMM altitude. The radar altitude value may be erroneous in areas of heavy
COMM tree cover, where the altimeter reflects the distance to the tree
COMM canopy rather than the ground. The GPS altitude value is primarily
COMM dependent on the number of available satellites. Although
COMM post-processing of GPS data will yield X and Y accuracies in the
COMM order of 1-2 metres, the accuracy of the altitude value is usually
COMM much less, sometimes in the ±5 metre range. Further inaccuracies
COMM may be introduced during the interpolation and gridding process.
COMM Because of the inherent inaccuracies of this method, no guarantee is
COMM made or implied that the information displayed is a true
COMM representation of the height above sea level. Although this product
COMM may be of some use as a general reference,
COMM THIS PRODUCT MUST NOT BE USED FOR NAVIGATION PURPOSES.
COMM -----
COMM
COMM ELECTROMAGNETIC SYSTEM
COMM
COMM TEMPEST IS A TIME-DOMAIN SQUARE-WAVE SYSTEM,
COMM TRANSMITTING AT A BASE FREQUENCY OF 25Hz,
COMM WITH 2 ORTHOGONAL-AXIS RECEIVER COILS IN A TOWED BIRD.
COMM FINAL EM OUTPUT IS RECORDED 5 TIMES PER SECOND.
COMM THE TIMES (IN MILLISECONDS) FOR THE 15 WINDOWS ARE:
COMM
COMM WINDOW      START      END      CENTRE
COMM    1         0.007     0.020     0.013
COMM    2         0.033     0.047     0.040
COMM    3         0.060     0.073     0.067

```

COMM	4	0.087	0.127	0.107
COMM	5	0.140	0.207	0.173
COMM	6	0.220	0.340	0.280
COMM	7	0.353	0.553	0.453
COMM	8	0.567	0.873	0.720
COMM	9	0.887	1.353	1.120
COMM	10	1.367	2.100	1.733
COMM	11	2.113	3.273	2.693
COMM	12	3.287	5.113	4.200
COMM	13	5.127	7.993	6.560
COMM	14	8.007	12.393	10.200
COMM	15	12.407	19.993	16.200

COMM

COMM PULSE WIDTH: 10 ms

COMM

COMM TEMPEST EM data are transformed to the response that would be  
 COMM obtained with a B-field sensor for a 100% duty cycle square  
 COMM waveform at the base frequency, involving a 1A change in  
 COMM current (from -0.5A to +0.5A to -0.5A) in a 1sq.m transmitter.  
 COMM It is this configuration, rather than the actual acquisition  
 COMM configuration, which must be specified when modelling TEMPEST data.  
 COMM  
 COMM

## LOCATED DATA FORMAT

Output field format : DOS - Flat ascii  
 Number of fields : 198

Field	Channel	Description	Units	Undefined
Format				
1	LINE	Line		-9999999 i6
2	FLIGHT	Flight		-9999999 i4
3	FID	Fiducial	(s)	-9999999 f8.1
4	LATITUDE	Latitude GDA94	(deg)	-9999999 f13.6
5	LONGITUDE	Longitude GDA94	(deg)	-9999999 f13.6
6	EASTING	Easting MGA53	(m)	-9999999 f11.2
7	NORTHING	Northing MGA53	(m)	-9999999 f12.2
8	TxHeight	GPS height	(m)	-9999999 f8.2
9	Baro	Barometric Altitude	(m)	-9999999 f8.2
10	TxRalt_raw	Raw Radar Altimeter	(m)	-9999999 f8.2
11	TxRalt_final	Final Radar Altimeter	(m)	-9999999 f8.2
12	DTM	DTM	(m)	-9999999 f8.2
13	MAG	Compensated TMI	(nT)	-9999999 f10.3
14	MAG_1VD	Levelled TMI 1VD	(nT/m)	-9999999 f12.5
15	Pitch_Raw	Raw Tx loop pitch	(deg)	-9999999 f10.5
16	Roll_Raw	Raw Tx loop roll	(deg)	-9999999 f10.5
17	HSep_Raw	Raw Tx-Rx horizontal separation	(m)	-9999999 f8.2
18	VSep_Raw	Raw Tx-Rx vertical separation	(m)	-9999999 f8.2
19	Pitch_Final	Final Tx loop pitch	(deg)	-9999999 f10.5
20	Roll_Final	Final Tx loop roll	(deg)	-9999999 f10.5
21	HSep_Final	Final Tx-Rx horizontal separation	(m)	-9999999 f8.2
22	VSep_Final	Final Tx-Rx vertical separation	(m)	-9999999 f8.2
23	EMX_Raw[1]	Raw EMX01 Window	(fT)	-9999999 f12.6
24	EMX_Raw[2]	Raw EMX02 Window	(fT)	-9999999 f12.6
25	EMX_Raw[3]	Raw EMX03 Window	(fT)	-9999999 f12.6
26	EMX_Raw[4]	Raw EMX04 Window	(fT)	-9999999 f12.6
27	EMX_Raw[5]	Raw EMX05 Window	(fT)	-9999999 f12.6
28	EMX_Raw[6]	Raw EMX06 Window	(fT)	-9999999 f12.6
29	EMX_Raw[7]	Raw EMX07 Window	(fT)	-9999999 f12.6
30	EMX_Raw[8]	Raw EMX08 Window	(fT)	-9999999 f12.6
31	EMX_Raw[9]	Raw EMX09 Window	(fT)	-9999999 f12.6

32	EMX_Raw[10]	Raw EMX10 Window	(fT)	-9999999	f12.6
33	EMX_Raw[11]	Raw EMX11 Window	(fT)	-9999999	f12.6
34	EMX_Raw[12]	Raw EMX12 Window	(fT)	-9999999	f12.6
35	EMX_Raw[13]	Raw EMX13 Window	(fT)	-9999999	f12.6
36	EMX_Raw[14]	Raw EMX14 Window	(fT)	-9999999	f12.6
37	EMX_Raw[15]	Raw EMX15 Window	(fT)	-9999999	f12.6
38	EMX_Final[1]	Final EMX01 Window	(fT)	-9999999	f12.6
39	EMX_Final[2]	Final EMX02 Window	(fT)	-9999999	f12.6
40	EMX_Final[3]	Final EMX03 Window	(fT)	-9999999	f12.6
41	EMX_Final[4]	Final EMX04 Window	(fT)	-9999999	f12.6
42	EMX_Final[5]	Final EMX05 Window	(fT)	-9999999	f12.6
43	EMX_Final[6]	Final EMX06 Window	(fT)	-9999999	f12.6
44	EMX_Final[7]	Final EMX07 Window	(fT)	-9999999	f12.6
45	EMX_Final[8]	Final EMX08 Window	(fT)	-9999999	f12.6
46	EMX_Final[9]	Final EMX09 Window	(fT)	-9999999	f12.6
47	EMX_Final[10]	Final EMX10 Window	(fT)	-9999999	f12.6
48	EMX_Final[11]	Final EMX11 Window	(fT)	-9999999	f12.6
49	EMX_Final[12]	Final EMX12 Window	(fT)	-9999999	f12.6
50	EMX_Final[13]	Final EMX13 Window	(fT)	-9999999	f12.6
51	EMX_Final[14]	Final EMX14 Window	(fT)	-9999999	f12.6
52	EMX_Final[15]	Final EMX15 Window	(fT)	-9999999	f12.6
53	X_Sferics	X_Sferics		-9999999	f10.3
54	X_Lowfreq	X_Lowfreq		-9999999	f10.3
55	X_Powerline	X_Powerline		-9999999	f10.3
56	X_VLF1	X_18.2kHz		-9999999	f10.3
57	X_VLF2	X_19.8kHz		-9999999	f10.3
58	X_VLF3	X_21.4kHz		-9999999	f10.3
59	X_VLF4	X_22.2kHz		-9999999	f10.3
60	X_Geofact	X_Geometric factor		-9999999	f10.3
61	EMZ_Raw[1]	Raw EMZ01 Window	(fT)	-9999999	f12.6
62	EMZ_Raw[2]	Raw EMZ02 Window	(fT)	-9999999	f12.6
63	EMZ_Raw[3]	Raw EMZ03 Window	(fT)	-9999999	f12.6
64	EMZ_Raw[4]	Raw EMZ04 Window	(fT)	-9999999	f12.6
65	EMZ_Raw[5]	Raw EMZ05 Window	(fT)	-9999999	f12.6
66	EMZ_Raw[6]	Raw EMZ06 Window	(fT)	-9999999	f12.6
67	EMZ_Raw[7]	Raw EMZ07 Window	(fT)	-9999999	f12.6
68	EMZ_Raw[8]	Raw EMZ08 Window	(fT)	-9999999	f12.6
69	EMZ_Raw[9]	Raw EMZ09 Window	(fT)	-9999999	f12.6
70	EMZ_Raw[10]	Raw EMZ10 Window	(fT)	-9999999	f12.6
71	EMZ_Raw[11]	Raw EMZ11 Window	(fT)	-9999999	f12.6
72	EMZ_Raw[12]	Raw EMZ12 Window	(fT)	-9999999	f12.6
73	EMZ_Raw[13]	Raw EMZ13 Window	(fT)	-9999999	f12.6
74	EMZ_Raw[14]	Raw EMZ14 Window	(fT)	-9999999	f12.6
75	EMZ_Raw[15]	Raw EMZ15 Window	(fT)	-9999999	f12.6
76	EMZ_Final[1]	Final EMZ01 Window	(fT)	-9999999	f12.6
77	EMZ_Final[2]	Final EMZ02 Window	(fT)	-9999999	f12.6
78	EMZ_Final[3]	Final EMZ03 Window	(fT)	-9999999	f12.6
79	EMZ_Final[4]	Final EMZ04 Window	(fT)	-9999999	f12.6
80	EMZ_Final[5]	Final EMZ05 Window	(fT)	-9999999	f12.6
81	EMZ_Final[6]	Final EMZ06 Window	(fT)	-9999999	f12.6
82	EMZ_Final[7]	Final EMZ07 Window	(fT)	-9999999	f12.6
83	EMZ_Final[8]	Final EMZ08 Window	(fT)	-9999999	f12.6
84	EMZ_Final[9]	Final EMZ09 Window	(fT)	-9999999	f12.6
85	EMZ_Final[10]	Final EMZ10 Window	(fT)	-9999999	f12.6
86	EMZ_Final[11]	Final EMZ11 Window	(fT)	-9999999	f12.6
87	EMZ_Final[12]	Final EMZ12 Window	(fT)	-9999999	f12.6
88	EMZ_Final[13]	Final EMZ13 Window	(fT)	-9999999	f12.6
89	EMZ_Final[14]	Final EMZ14 Window	(fT)	-9999999	f12.6
90	EMZ_Final[15]	Final EMZ15 Window	(fT)	-9999999	f12.6
91	Z_Sferics	Z_Sferics		-9999999	f10.3
92	Z_Lowfreq	Z_Lowfreq		-9999999	f10.3
93	Z_Powerline	Z_Powerline		-9999999	f10.3
94	Z_VLF1	Z_18.2kHz		-9999999	f10.3
95	Z_VLF2	Z_19.8kHz		-9999999	f10.3

96	Z_VLF3	Z_21.4kHz				-9999999	f10.3
97	Z_VLF4	Z_22.2kHz				-9999999	f10.3
98	Z_Geofact	Z_Geometric factor				-9999999	f10.3
99	CNDX[1]	Conductivity_X001	0-2	m	(mS/m)	-9999999	f10.3
100	CNDX[2]	Conductivity_X002	2-4	m	(mS/m)	-9999999	f10.3
101	CNDX[3]	Conductivity_X003	4-6	m	(mS/m)	-9999999	f10.3
102	CNDX[4]	Conductivity_X004	6-8	m	(mS/m)	-9999999	f10.3
103	CNDX[5]	Conductivity_X005	8-10	m	(mS/m)	-9999999	f10.3
104	CNDX[6]	Conductivity_X006	10-12	m	(mS/m)	-9999999	f10.3
105	CNDX[7]	Conductivity_X007	12-14	m	(mS/m)	-9999999	f10.3
106	CNDX[8]	Conductivity_X008	14-16	m	(mS/m)	-9999999	f10.3
107	CNDX[9]	Conductivity_X009	16-18	m	(mS/m)	-9999999	f10.3
108	CNDX[10]	Conductivity_X010	18-20	m	(mS/m)	-9999999	f10.3
109	CNDX[11]	Conductivity_X011	20-22	m	(mS/m)	-9999999	f10.3
110	CNDX[12]	Conductivity_X012	22-24	m	(mS/m)	-9999999	f10.3
111	CNDX[13]	Conductivity_X013	24-26	m	(mS/m)	-9999999	f10.3
112	CNDX[14]	Conductivity_X014	26-28	m	(mS/m)	-9999999	f10.3
113	CNDX[15]	Conductivity_X015	28-30	m	(mS/m)	-9999999	f10.3
114	CNDX[16]	Conductivity_X016	30-32	m	(mS/m)	-9999999	f10.3
115	CNDX[17]	Conductivity_X017	32-34	m	(mS/m)	-9999999	f10.3
116	CNDX[18]	Conductivity_X018	34-36	m	(mS/m)	-9999999	f10.3
117	CNDX[19]	Conductivity_X019	36-38	m	(mS/m)	-9999999	f10.3
118	CNDX[20]	Conductivity_X020	38-40	m	(mS/m)	-9999999	f10.3
119	CNDX[21]	Conductivity_X021	40-42	m	(mS/m)	-9999999	f10.3
120	CNDX[22]	Conductivity_X022	42-44	m	(mS/m)	-9999999	f10.3
121	CNDX[23]	Conductivity_X023	44-46	m	(mS/m)	-9999999	f10.3
122	CNDX[24]	Conductivity_X024	46-48	m	(mS/m)	-9999999	f10.3
123	CNDX[25]	Conductivity_X025	48-50	m	(mS/m)	-9999999	f10.3
124	CNDX[26]	Conductivity_X026	50-52	m	(mS/m)	-9999999	f10.3
125	CNDX[27]	Conductivity_X027	52-54	m	(mS/m)	-9999999	f10.3
126	CNDX[28]	Conductivity_X028	54-56	m	(mS/m)	-9999999	f10.3
127	CNDX[29]	Conductivity_X029	56-58	m	(mS/m)	-9999999	f10.3
128	CNDX[30]	Conductivity_X030	58-60	m	(mS/m)	-9999999	f10.3
129	CNDX[31]	Conductivity_X031	60-62	m	(mS/m)	-9999999	f10.3
130	CNDX[32]	Conductivity_X032	62-64	m	(mS/m)	-9999999	f10.3
131	CNDX[33]	Conductivity_X033	64-66	m	(mS/m)	-9999999	f10.3
132	CNDX[34]	Conductivity_X034	66-68	m	(mS/m)	-9999999	f10.3
133	CNDX[35]	Conductivity_X035	68-70	m	(mS/m)	-9999999	f10.3
134	CNDX[36]	Conductivity_X036	70-72	m	(mS/m)	-9999999	f10.3
135	CNDX[37]	Conductivity_X037	72-74	m	(mS/m)	-9999999	f10.3
136	CNDX[38]	Conductivity_X038	74-76	m	(mS/m)	-9999999	f10.3
137	CNDX[39]	Conductivity_X039	76-78	m	(mS/m)	-9999999	f10.3
138	CNDX[40]	Conductivity_X040	78-80	m	(mS/m)	-9999999	f10.3
139	CNDX[41]	Conductivity_X041	80-82	m	(mS/m)	-9999999	f10.3
140	CNDX[42]	Conductivity_X042	82-84	m	(mS/m)	-9999999	f10.3
141	CNDX[43]	Conductivity_X043	84-86	m	(mS/m)	-9999999	f10.3
142	CNDX[44]	Conductivity_X044	86-88	m	(mS/m)	-9999999	f10.3
143	CNDX[45]	Conductivity_X045	88-90	m	(mS/m)	-9999999	f10.3
144	CNDX[46]	Conductivity_X046	90-92	m	(mS/m)	-9999999	f10.3
145	CNDX[47]	Conductivity_X047	92-94	m	(mS/m)	-9999999	f10.3
146	CNDX[48]	Conductivity_X048	94-96	m	(mS/m)	-9999999	f10.3
147	CNDX[49]	Conductivity_X049	96-98	m	(mS/m)	-9999999	f10.3
148	CNDX[50]	Conductivity_X050	98-100	m	(mS/m)	-9999999	f10.3
149	CNDX[51]	Conductivity_X051	100-102	m	(mS/m)	-9999999	f10.3
150	CNDX[52]	Conductivity_X052	102-104	m	(mS/m)	-9999999	f10.3
151	CNDX[53]	Conductivity_X053	104-106	m	(mS/m)	-9999999	f10.3
152	CNDX[54]	Conductivity_X054	106-108	m	(mS/m)	-9999999	f10.3
153	CNDX[55]	Conductivity_X055	108-110	m	(mS/m)	-9999999	f10.3
154	CNDX[56]	Conductivity_X056	110-112	m	(mS/m)	-9999999	f10.3
155	CNDX[57]	Conductivity_X057	112-114	m	(mS/m)	-9999999	f10.3
156	CNDX[58]	Conductivity_X058	114-116	m	(mS/m)	-9999999	f10.3
157	CNDX[59]	Conductivity_X059	116-118	m	(mS/m)	-9999999	f10.3
158	CNDX[60]	Conductivity_X060	118-120	m	(mS/m)	-9999999	f10.3
159	CNDX[61]	Conductivity_X061	120-122	m	(mS/m)	-9999999	f10.3

160	CNDX[62]	Conductivity_X062	122-124 m	(mS/m)	-9999999	f10.3
161	CNDX[63]	Conductivity_X063	124-126 m	(mS/m)	-9999999	f10.3
162	CNDX[64]	Conductivity_X064	126-128 m	(mS/m)	-9999999	f10.3
163	CNDX[65]	Conductivity_X065	128-130 m	(mS/m)	-9999999	f10.3
164	CNDX[66]	Conductivity_X066	130-132 m	(mS/m)	-9999999	f10.3
165	CNDX[67]	Conductivity_X067	132-134 m	(mS/m)	-9999999	f10.3
166	CNDX[68]	Conductivity_X068	134-136 m	(mS/m)	-9999999	f10.3
167	CNDX[69]	Conductivity_X069	136-138 m	(mS/m)	-9999999	f10.3
168	CNDX[70]	Conductivity_X070	138-140 m	(mS/m)	-9999999	f10.3
169	CNDX[71]	Conductivity_X071	140-142 m	(mS/m)	-9999999	f10.3
170	CNDX[72]	Conductivity_X072	142-144 m	(mS/m)	-9999999	f10.3
171	CNDX[73]	Conductivity_X073	144-146 m	(mS/m)	-9999999	f10.3
172	CNDX[74]	Conductivity_X074	146-148 m	(mS/m)	-9999999	f10.3
173	CNDX[75]	Conductivity_X075	148-150 m	(mS/m)	-9999999	f10.3
174	CNDX[76]	Conductivity_X076	150-152 m	(mS/m)	-9999999	f10.3
175	CNDX[77]	Conductivity_X077	152-154 m	(mS/m)	-9999999	f10.3
176	CNDX[78]	Conductivity_X078	154-156 m	(mS/m)	-9999999	f10.3
177	CNDX[79]	Conductivity_X079	156-158 m	(mS/m)	-9999999	f10.3
178	CNDX[80]	Conductivity_X080	158-160 m	(mS/m)	-9999999	f10.3
179	CNDX[81]	Conductivity_X081	160-162 m	(mS/m)	-9999999	f10.3
180	CNDX[82]	Conductivity_X082	162-164 m	(mS/m)	-9999999	f10.3
181	CNDX[83]	Conductivity_X083	164-166 m	(mS/m)	-9999999	f10.3
182	CNDX[84]	Conductivity_X084	166-168 m	(mS/m)	-9999999	f10.3
183	CNDX[85]	Conductivity_X085	168-170 m	(mS/m)	-9999999	f10.3
184	CNDX[86]	Conductivity_X086	170-172 m	(mS/m)	-9999999	f10.3
185	CNDX[87]	Conductivity_X087	172-174 m	(mS/m)	-9999999	f10.3
186	CNDX[88]	Conductivity_X088	174-176 m	(mS/m)	-9999999	f10.3
187	CNDX[89]	Conductivity_X089	176-178 m	(mS/m)	-9999999	f10.3
188	CNDX[90]	Conductivity_X090	178-180 m	(mS/m)	-9999999	f10.3
189	CNDX[91]	Conductivity_X091	180-182 m	(mS/m)	-9999999	f10.3
190	CNDX[92]	Conductivity_X092	182-184 m	(mS/m)	-9999999	f10.3
191	CNDX[93]	Conductivity_X093	184-186 m	(mS/m)	-9999999	f10.3
192	CNDX[94]	Conductivity_X094	186-188 m	(mS/m)	-9999999	f10.3
193	CNDX[95]	Conductivity_X095	188-190 m	(mS/m)	-9999999	f10.3
194	CNDX[96]	Conductivity_X096	190-192 m	(mS/m)	-9999999	f10.3
195	CNDX[97]	Conductivity_X097	192-194 m	(mS/m)	-9999999	f10.3
196	CNDX[98]	Conductivity_X098	194-196 m	(mS/m)	-9999999	f10.3
197	CNDX[99]	Conductivity_X099	196-198 m	(mS/m)	-9999999	f10.3
198	CNDX[100]	Conductivity_X100	198-200 m	(mS/m)	-9999999	f10.3

COMM

Total number of lines : 12

COMM

COMM	Flt	Line	Start X	Start Y	End X	End Y	Kms
COMM	2	10010	290085	7491956	290091	7440390	51.57
COMM	2	10023	274958	7439776	274947	7491899	52.12
COMM	2	10031	264993	7491936	264995	7439962	51.97
COMM	2	10040	255038	7439834	255039	7476774	36.94
COMM	2	10052	244852	7476645	245004	7439963	36.68
COMM	1	10060	234975	7439916	234991	7481987	42.07
COMM	1	10070	225015	7468996	225021	7439838	29.16
COMM	1	10080	214998	7451740	214998	7468622	16.88
COMM	1	10090	204976	7468595	204964	7451684	16.91
COMM	1	10100	194992	7439986	195005	7464775	24.79
COMM	2	10110	226929	7474977	299347	7475163	72.42
COMM	1	10120	299897	7444853	181852	7444875	118.04

COMM

Total Kilometres : 549.56

## APPENDIX V – List of all Supplied Data and Products

### Final Located Data

**\*\* Each client received a copy of their own data and the combined data**

Southern\_NT\_Toro.hdr - header file describing the contents of...

Southern\_NT\_Toro.asc - flat ascii file containing located magnetic, EM and elevation data (see App IV).

Southern\_NT\_Toro.gdb - Geosoft GDB file containing located magnetic, EM and elevation data (see App IV).

Southern\_NT\_Scimitar.hdr - header file describing the contents of...

Southern\_NT\_Scimitar.asc - flat ascii file containing located magnetic, EM and elevation data (see App IV).

Southern\_NT\_Scimitar.gdb - Geosoft GDB file containing located magnetic, EM and elevation data (see App IV).

Southern\_NT\_combined.hdr - header file describing the contents of...

Southern\_NT\_combined.asc - flat ascii file containing located magnetic, EM and elevation data (see App IV).

Southern\_NT\_combined.gdb - Geosoft GDB file containing located magnetic, EM and elevation data (see App IV).

### Final Digital Products

- Flight Path
- Conductivity Depth Image Multiplots & Stacked sections X-component

### Final Acquisition and Processing Report

Delivered as hardcopy and digitally